Atmos. Chem. Phys. Discuss., 15, 16985–17050, 2015
www.atmos-chem-phys-discuss.net/15/16985/2015/
doi:10.5194/acpd-15-16985-2015
© Author(s) 2015. CC Attribution 3.0 License.

Atmospheric Chemistry and Physics
Open Access
Discussions

This discussion paper is/has been under review for the journal Atmospheric Chemistry and Physics (ACP). Please refer to the corresponding final paper in ACP if available.

Spatiotemporal variations of air pollutants (O_3, NO_2, SO_2, CO, PM_{10}, and VOCs) with land-use types

J.-M. Yoo[1], M.-J. Jeong[2], D. Kim[3], W. R. Stockwell[4], J.-H. Yang[5], H.-W. Shin[2], M.-I. Lee[6], C.-K. Song[7], and S.-D. Lee[7]

[1]Dept. of Science Education, Ewha Womans University, Seoul, Republic of Korea
[2]Dept. of Atmospheric and Environmental Sciences, Gangneung-Wonju National University, Gangneung, Gangwon-do, Republic of Korea
[3]Universities Space Research Association, Columbia, MD, USA
[4]Dept. of Chemistry, Howard University, Washington, D.C., USA
[5]Dept. of Atmospheric Science and Engineering, Ewha Womans University, Seoul, Republic of Korea
[6]School of Urban and Environmental Engineering, Ulsan National Institute of Science and Technology, Ulsan, Republic of Korea
[7]National Institute of Environmental Research, Incheon, Republic of Korea

Received: 25 May 2015 – Accepted: 01 June 2015 – Published: 22 June 2015

Correspondence to: M.-J. Jeong (mjeong@gwnu.ac.kr)

Published by Copernicus Publications on behalf of the European Geosciences Union.

ACPD

15, 16985–17050, 2015

Spatiotemporal variations of air pollutants with land-use types

J.-M. Yoo et al.

Abstract

The spatiotemporal variations of surface air pollutants (O_3, NO_2, SO_2, CO, and PM_{10}) with four land-use types: residence (R), commerce (C), industry (I) and greenbelt (G) have been investigated at 283 stations in South Korea during 2002–2013, using routinely observed data. The VOCs data at 9 photochemical pollutant monitoring stations available since 2007 were utilized in order to examine their effect on the ozone chemistry. The land-use types, set by the Korean government, were generally consistent with the satellite-derived land covers and with the previous result showing anti-correlation between O_3 and NO_2 in diverse urban areas. The relationship between the two pollutants in the Seoul Metropolitan Area (SMA) residence land-use areas was substantially different from that outside of the SMA, probably due to the local differences in vehicle emissions. The highest concentrations of air pollutants in the diurnal, weekly, and annual cycles were found in industry for SO_2 and PM_{10}, in commerce for NO_2 and CO, and in greenbelt for O_3, respectively. The concentrations of air pollutants, except for O_3, were generally higher in big cities during weekdays while O_3 showed its peak in suburban areas or small cities during weekends. The weekly cycle and trends of O_3 were significantly out of phase with those of NO_2, particularly in the residential and commercial areas, suggesting that vehicle emission was a major source in those areas. The ratios of VOCs to NO_2 for each of the land-use types were in the order of I (10.2) > C (8.7) > G (3.9) > R (3.6), suggesting that most areas in South Korea were likely to be VOCs-limited for ozone chemistry. The pollutants (NO_2, SO_2, CO, and PM_{10}) except for O_3 have decreased most likely due to the effective government control. The total oxidant values ($OX = O_3 + NO_2$) with the land-use types were analyzed for the local and regional (or background) contributions of O_3, respectively, and the order of OX (ppb) was C (57.4) > R (53.6) > I (50.7) > G (45.4), indicating the greenbelt observation was close to the background.

ACPD
15, 16985–17050, 2015

Spatiotemporal variations of air pollutants with land-use types

J.-M. Yoo et al.

1 Introduction

The spatiotemporal variations in major air pollutants with the land-use types in urban or suburban areas (e.g., Kuttler and Strassburger, 1999 for O_3 and NO_2; Flemming et al., 2005 for O_3, NO_2, SO_2, and PM_{10}) are of great interest in densely-populated South Korea because the pollutants from local, regional, and global sources can have an impact on human health and ecosystems (e.g., Cooper et al., 2010 for O_3; Gilge et al., 2010; Kim et al., 2011 for PM_{10}; Valks et al., 2011 for NO_2), and on climate change (WMO, 2007). The major surface air pollutants examined in this study were ozone (O_3), nitrogen dioxide (NO_2), sulfur dioxide (SO_2), carbon monoxide (CO), particulate matter (PM_{10}) and volatile organic compounds (VOCs). Due to the high energy consumption of South Korea, the country was expected to produce substantial amounts of domestic anthropogenic pollutants (Kim et al., 2013a).

Since air pollutants could be transported from industrialized China to Korea (e.g., Zhang et al., 2009; Kim et al., 2011 for NO_x; Wang et al., 2013 for NO_x and SO_2), their trends and characteristics need to be analyzed in view of international cooperation in reducing the pollutants. The impact of pollutants on a certain area can be associated with its population and emission controls, etc. (Meng et al., 2009). In order to improve the air quality in South Korea, the Ministry of Environment of Korea (MEK) monitored the major pollutants with four land-use types (residence, commerce, industry and greenbelt) set by the Ministry of Land, Infrastructure and Transport (MLIT). Please see Table 1 for the abbreviations in this study. Since the anthropogenic sources of air pollutants, such as transportation and industrial complexes, vary locally with the land-use types, it was more efficient to investigate the spatiotemporal variations of the constituents with the land-use types for our comprehensive analysis and for ultimately controlling them.

Among the major pollutants, CO, nitrogen oxides ($NO_x = NO + NO_2$), PM_{10}, and some types of VOCs (e.g., BTEX; benzene, toluene, ethylbenzene, and ortho-, meta-, and para-xylenes) are primarily traffic-induced while O_3 and NO_2 are secondary trace

ACPD
15, 16985–17050, 2015

CC BY

gases formed from precursors in photochemical reactions (e.g., Kuttler and Strussburger, 1999; Masiol et al., 2014). The main sources of SO_2, the most important precursor for acid rain (Wang and Wang, 1995; Wang et al., 2001), are power plants and heavy industry. The formation of ground level O_3 also depends on the influx of stratospheric O_3, the concentrations of NO_x, NO_y (i.e., the family of reactive nitrogen species; Pandey Deolal et al., 2012), VOCs, and the ratio of VOCs to NO_x (Nevers, 2000). When the ratio of VOCs to NO_x is less than 8 to 10, decreasing NO_x tends to increase ozone formation (VOC-limited or VOC-sensitive, Larsen et al., 2003; Qin et al., 2004a). On the other hand, when the ratio is higher than 8 to 10, decreasing NO_x tends to decrease ozone formation (NO_x-limited or NO_x-sensitive). However, the value may change due to various factors (e.g., meteorology, deposition, and gas to particle conversion) (Jacobson, 2002).

Nitrogen dioxides have a substantial impact on PM_{10} through their atmospheric oxidation to aerosol nitrate, and the CO formed from the oxidation of VOCs (e.g., Wang et al., 2008), and the NO_2 emissions due to most types of anthropogenic combustion are a major O_3 precursor (Gilge et al., 2010; Lamsal et al., 2010, 2011). The SO_2 also leads to photochemical O_3 production with the NO_x and VOCs under the intense insolation (Klemm et al., 2000; Derwent et al., 2003). In other words, the photochemistry of NO-NO_2-O_3 system in the tropospheric surface layer is locally controlled by the reactions with CO and many VOCs and even SO_2 (Derwent et al., 2003; Masiol et al., 2014). Meanwhile, the PM_{10} aerosol, and the SO_2 and NO_2 gases may act as condensation nuclei or affect the formation of cloud particles in hydrological circulation (Bian et al., 2007 for PM_{10}). The PM_{10} concentrations can affect UV flux and O_3 formation (Qin et al., 2004b; Bian et al., 2007; Han et al., 2011). Therefore, controlling over the amount of O_3 is difficult due to non-linear features of its formation reactions (Mazzeo et al., 2005; Jin et al., 2012). In particular, spatiotemporal variations of O_3 in South Korea have not been fully understood yet. Overall, the reactions or interactions of the above pollutants are multiple and complex.

ACPD
15, 16985–17050, 2015

Masiol et al. (2014) reported on the trends and cycles of the pollutants (O_3, NO_2, SO_2, CO, PM_{10}, and BTEX) in a large city in northern Italy and they discussed their interactions. There have been dozens of previous studies on the spatiotemporal variations of some substances among the major air pollutants in terms of their cycles (diurnal, weekly and annual) and trends over South Korea. The cycles of each of the pollutants are helpful in order to understand the emission sources, human activities, photochemical processes and meteorological factors that affect it (e.g., Flemming et al., 2005; Meng et al., 2009). Seo et al. (2014) reported that the O_3 trend in South Korea from 1999 to 2010 was similar to that of NO_2 and it increased by +0.26 ppbv yr^{-1} possibly due to the local increase in anthropogenic precursor emissions and meteorological effects. Based on a model simulation, Jin et al. (2012) showed that the Seoul Metropolitan Area (SMA) was VOCs-limited for the O_3 control, while the local province outside the SMA was chemistry between VOCs-limited and NO_x-limited. However, Kim et al. (2013b) reported that in the suburban SMA, the biogenic VOCs could be the most important source of high O_3 episodes. The temporal O_3 averages in the SMA and other inland areas were low as a result of an increase in O_3 titration by NO from enhanced NO_x levels compared to those at the coastal areas sometimes due to a land–sea breeze (Ghim and Chang, 2000; Oh et al., 2006; Seo et al., 2014). In other words, the titration can slow down the O_3 accumulation in the urban (or suburban) areas due to significant concentrations of NO (Chou et al., 2006).

The long-term NO_2 trends in South Korea from 1998 to 2008 were different between Seoul and other cites with more declining trends at the Seoul sites (Shon and Kim, 2011), presumably due to the MEK effort to reduce the NO_x emissions from the SMA (Kim et al., 2013a). Diurnal and seasonal variations in the individual VOCs at a site in Seoul in 2004 were measured by Nguyen et al. (2009), provided information on the relative abundance of anthropogenic emissions compared to natural emissions. Long-term changes in the PM_{10} in South Korea in some periods between 1992 and 2010 were reported in urban areas by Kim and Shon (2011), and Sharma et al. (2014), and at the background site of Gosan by Kim et al. (2011). Meanwhile, Flemming et al. (2005)

CC BY

investigated the cycles of the four air pollutants (O_3, NO_2, SO_2, and PM_{10}) in Germany based on an objective air quality classification scheme of hierarchical clustering.

The weekend effect, derived from the weekly cycle, has been focused primarily on the relationship between O_3 and NO_2 in many previous studies (e.g., Brönnimann et al., 2000; Fujita et al., 2003a, b; Beirle et al., 2003; Qin et al., 2004b). In these studies, they examined the weekend effect because it can be an indicator of urbanization or human activity (Atkinson-Palombo et al., 2006). For instance, the analysis of the NO_x weekly cycle could be useful in discriminating between its anthropogenic (e.g., local traffic) and natural sources (Beirle et al., 2003). The weekly cycles (or weekend/weekday effect) of O_3, NO_x, and VOCs provide insight into NO_x and VOCs limitation as well. Particularly, the analysis with the land-use types in our study can be helpful in estimating various kinds of man-made emissions (e.g., vehicles and factories, etc.). Despite relatively low concentrations of O_3 precursors (NO_x and VOCs) during the weekend, "high O_3 concentrations" at that time were observed in California (Marr and Harley, 2002a, b; Qin et al., 2004b), in remote areas (Brönnimann et al., 2000; Pudasainee et al., 2006), and in Japan (Sakamoto et al., 2005). In more detail, Beirle et al. (2003) examined the weekly cycle of the tropospheric NO_2 Vertical Column Densities (VCD) emitted by anthropogenic sources from a number of metropolises throughout the world, using satellite data from the Global Ozone Monitoring Experiment (GOME) during the 1996–2001 period. According to their report, NO_2 concentration tended to decrease on weekends when human activity was relatively low. Qin et al. (2004b) revealed that in southern California, the VOCs sensitivity at weekend, accompanied with the reduced NO_x and PM_{10} emissions, could result in enhanced O_3 formation, although this tendency was not shown in some areas close to the beach and far downstream from L.A. downtown. This result suggests that the weekend effect may vary with meteorological factors (e.g., Jacobson, 2002) and land-use types. A study on their reactive relationship (O_3, NO_2, and VOCs) with the land-use types in South Korea is required in order to explain the possible causes for the O_3 formation and to make a policy decision for either NO_x-limited or VOCs-limited regimes for the formation over the country.

ACPD
15, 16985–17050, 2015

cc BY

As we mentioned earlier, the spatiotemporal analyses of some species among the major air pollutants have been assessed in many previous studies in terms of their cycles, trends, and interactions, although the VOCs analyses are still lacking due to the limited observations and data. To the best of our knowledge, there have not been any comprehensive studies on the spatiotemporal variation of the major air pollutants at 283 stations over South Korea associated with land-use types (i.e., residence, commerce, industry, and greenbelt areas), using simultaneous measurement data from a dense observational network. The VOC data available since 2007 have also been utilized to examine the relative influences of VOCs and NO_2 on the O_3 change. A large number of data on the $0.1^{\circ} \times 0.1^{\circ}$ or $0.25^{\circ} \times 0.25^{\circ}$ spatial grids were developed to better understand the spatiotemporal variations of the pollutants with the types requires high quality, long-term observations of these reactive substances.

The purpose of this study was to comprehensively investigate the spatiotemporal variations and their consistency of the major pollutants (O_3, NO_2, SO_2, CO, PM_{10}, and VOCs) over the four land-use types in terms of their cycles (diurnal, weekly, and annual), trends, and relationships, based on simultaneous hourly observations at the stations located in urban or suburban areas in South Korea. In Sect. 2, we briefly describe the data and measurements of the pollutants. In addition, we introduce the indices of the land surface properties derived from the satellite data to compare the four land-use types of the MEK. In Sect. 3, the climatological pollutant averages are given for the seasons and the land-use types, respectively. The results for their cycles and trends are described in Sects. 4 and 5, respectively. We investigate the relationship between O_3 and NO_2 with the land-use types and discuss the results in Sect. 6, and the weekend effect (O_3, NO_2 and VOCs) in Sect. 7. Finally, the conclusions are provided in Sect. 8.

ACPD
15, 16985–17050, 2015

CC BY

2 Data and method

The information for the surface air pollutants (O_3, CO, NO_2, SO_2, PM_{10} and VOCs) data used in this study is presented in Table 2. Hereinafter the four pollutants (CO, NO_2, SO_2, and PM_{10}) will be called "the CNSP pollutants" in this study. The above pollutants except VOCs have been measured each hour at 283 air pollution monitoring stations of the MEK in South Korea during the period from January 2002 to December 2013 (Fig. 1a–d), while the VOCs data at 19 stations were available since 2007. The majority of observational sites were located in urban or suburban areas rather than remote areas. These pollutants were predominantly produced by mobile and stationary combustion, and/or photochemical processes (Masiol et al., 2014). The pollutants, except for VOCs, were investigated as time-averaged in the two spatial grids ($0.1° \times 0.1°$ and $0.25° \times 0.25°$) after categorizing the 283 site data into the four land-use types as follows: 154 residential (R), 57 commercial (C), 35 industrial (I) and 37 greenbelt (G) stations (see Tables 1–2 for details).

The MLIT classified the land of South Korea into these types in order to enhance the efficiency of land-use. According to Article 36 of the National Land Planning and Utilization Act (http://www.law.go.kr/engLsSc.do?menuId=0&subMenu=5&query=NATIONAL_LAND_PLANNING_AND_UTILIZATION_ACT#liBgcolor2), urban or suburban areas are designated under any of the following categories: (a) Residential areas (i.e., Residence) necessary in order to protect peaceful dwelling and sound living environment, (b) Commercial areas (i.e., Commerce) necessary to increase convenience for commerce and other businesses, (c) Industrial areas (i.e., Industry) necessary to increase the convenience of industries; and (d) Green areas (i.e., Greenbelt) requiring the conservation of green areas to protect the natural environment, farmland and forests, health and sanitation, security and to prevent any disorderly sprawl of cities. The areas of the four land-use types have been subdivided based on Article 30 of the Enforcement Decree of the National Land Planning and Utilization Act (Please see the above link at http://www.law.go.kr/, keyword: National Land Planning and Utiliza-

ACPD
15, 16985–17050, 2015

CC BY

tion Act). In addition the MLIT criteria for the types are available in the Supplement in Korean (http://www.law.go.kr/, keyword: National Land Planning and Utilization Act in Korean).

The higher spatial resolutions of the $0.1^\circ \times 0.1^\circ$ grid generally tended to represent the characteristics of big urban cities more than in suburban regions, when they were compared to those of coarser resolution (i.e., $0.25^\circ \times 0.25^\circ$). This is due to the fact that the stations were densely located in the former areas. Because of the difference in the numbers of stations in each grid, the grid numbers that returned the valid grid-averages of observations at the $0.1^\circ \times 0.1^\circ$ and $0.25^\circ \times 0.25^\circ$ resolutions with respect to the non-gridded 283 stations were reduced to 196 (R; 89, C; 42, I; 32, G; 33) for the $0.1^\circ \times 0.1^\circ$ and 146 (R; 59, C; 30, I; 25, G; 32) for the $0.25^\circ \times 0.25^\circ$ resolutions, respectively. Nine out of the 19 VOCs stations were selected in this study based on the criteria of better co-location of the observational sites and longer data records since 2007 (Table 2 and Fig. 1e). The VOCs at the 9 MEK photochemical stations were simultaneously observed with the other pollutants at the same sites.

The hourly observations of the pollutants, except for the VOCs, during the 12 year period were utilized for the temporal cycle and trend analyses over the land-use types. The hourly data were arranged into 144 monthly anomaly values in order to remove the annual cycle in the trend analyses (Fig. 7) and the scatter diagrams (Fig. 8). The anomaly value was computed by substracting the climatology (i.e., 12 year monthly mean in this study) from the monthly average in a given month. The 95 % confidence intervals for the trends were calculated using the bootstrap method (Wilks, 1995). For each air pollutant anomaly data set, 10 000 new data sets were created to produce 10 000 linear trends through random sampling (e.g., Lee et al., 2013). The random sampling was conducted by drawing data out of the respective original records of the air pollutant anomalies, allowing repetition. The ± values in the trend analysis defined the 95 % confidence intervals, while they stood for 1σ (standard deviation) in the concentration averages.

ACPD
15, 16985–17050, 2015

cc BY

The details of the surface air pollutants measurements including the instrumentation and methods are given in Table 3. Different instruments were employed to measure the pollutants. The O_3 concentrations were measured by Thermo 49i analyzers using the ultraviolet (UV) photometric method (e.g., Diaz-de-Quijano et al., 2009). The non-dispersive infrared method was utilized to measure the CO with Thermo, 48CTL which had been used near Beijing in Wang et al. (2008). The NO_2 was measured by Thermo, 42CTL using the chemiluminescence method. The Thermo, 43CTL was used to measure the SO_2, based on pulse UV fluorescence method. The PM_{10} was measured by Thermo, Model FH62-C14 (http://www.thermo.com) with the β-ray absorption method (e.g., Elbir et al., 2011). The control methods, which avoided high humidity (or condensation) in the measurement systems, were discussed in detail in Yoo et al. (2014).

For the VOC observations, the water vapor in the air samples, which were collected every hour, was removed from the air using a Nafion Dryer. A total of 56 VOC species were identified and quantified using a combination of the on-line thermal desorption system (Unity/Air Server, Markes) and the GC/Deans switch/Dual FID system (Varian 3800 GC, USA). These VOC compounds could be grouped into alkyne (1), aromatic (16), olefin (10), and paraffin (29) groups (Nguyen et al., 2009). The quality check for the GC was carefully calibrated, which was routinely conducted by site managers.

In order to approximately examine the validity of the four MEK land-use types at 283 sites in South Korea, we compared them with satellite derived land-covers of both the AVHRR and MODIS in a $0.25^{\circ} \times 0.25^{\circ}$ grid (Table 4). The AVHRR data were provided for 13 land covers over the globe at a 1 km × 1 km pixel resolution, time-averaged during 1981–1994 (e.g., De Fries et al., 1998; Hansen et al., 2000). The MODIS data were derived for 17 land covers over the globe at a 5 km × 5 km spatial resolution from 2002 to 2012 (e.g., Friedl et al., 2010), and they were available each year.

Although the land covers of both of the satellites were obtained from different periods, the AVHRR and MODIS original types were regrouped in this study and compared for the following four land covers: forest/woods, grass/shrub, urban/built-up, and water (Table 4). The MODIS "water" covers with the land-use types were not changed dur-

ACPD
15, 16985–17050, 2015

CC BY

ing the year period, and the covers were greater in the MEK "industry and greenbelt" types than in the "commerce and residence" types (Fig. 3d). In the table, the values with and without parentheses indicate the MODIS and AVHRR data, respectively. The MEK land-use types, set by the Korean government, were generally consistent with the satellite-derived land covers. The MEK "greenbelt" type compared to the three other types highly corresponded to the satellite-derived "forest/wood" (35.2–37.2 %) cover, but rarely to the "urban/build-up" (0–16.4 %). For AVHRR, the "water" like river dominated in the MEK types of "greenbelt" and "industry", while the "urban and built" matched well with the MEK "commerce" type (Fig. 2). The "industry" areas were expected to be located near rivers for transportation.

Figure 3 shows the interannual variations in the MODIS-derived land-cover types (%) vs. the MEK four land-use types from 2002 to 2012. The interannual variations in the MODIS land-covers with respect to the MEK types were not significant during that time period. It is reasonable that MODIS "forest/wood" covers were the greatest (37.2 %) in the MEK "greenbelt" type (Fig. 3a and Table 4). In the MEK "residence" type, the MODIS "forest/wood" cover was slightly increased, but the "grass/shrub" cover had decreased (Fig. 3a and b). The MODIS "urban/build-up" was at a minimum (16.4 %) in the MEK "greenbelt" and at a maximum (32.2 %) in the "commerce" (Fig. 3c and Table 4). In addition, the validity of the MEK types was investigated again in Sect. 7 of this study in terms of the relationship between O_3 and NO_2. The inverse relationship between the two variables over the various land-use types of urban areas has been studied significantly in previous studies (e.g., Kuttler and Strassburger, 1999, their Fig. 3; http://www.sciencetime.org/ConstructedClimates/chap-4-emissions-urban-air/3-9-complicated-ozone; Masiol et al., 2014, their Fig. 5).

ACPD
15, 16985–17050, 2015

CC BY

3 Climatological seasonal distributions of the pollutants: O_3, CO, SO_2, NO_2 and PM_{10}

Figure 4 shows the spatial distributions of the climatological seasonal averages of O_3 (ppb), CO (0.1 ppm), NO_2 (ppb), SO_2 (ppb) and PM_{10} ($\mu g\, m^{-3}$) in a $0.25° \times 0.25°$ grid over South Korea from 2002 to 2013. The seasonal and annual averages of the five pollutants are summarized in two different types of spatial grids ($0.25° \times 0.25°$ and $0.1° \times 0.1°$) in Table 5. In the table, the standard deviation (σ) values of the five pollutants are also presented with the ± values. The distributions were highly seasonal. The peak season of O_3 in South Korea was in the spring (March, April and May) than in the summer (June, July and August) due to the summertime monsoon and clouds. The O_3 level was the lowest in the winter due to the low photolysis (Table 5). Higher concentrations of the CNSP pollutants appeared in large cities (e.g., the SMA) more often than in suburban/rural areas. However, the O_3 values were lower over the large cities than over either their outer or coastal regions due to its reaction with other air pollutants and meteorological conditions (Seo et al., 2014). According to their study, the O_3 values over the large cities were low because of the NO titration even during the night without photochemical reactions by local anthropogenic precursor emissions, while they were high in the coastal areas because of the sea breeze effect. Since O_3 and NO do not coexist at night, NO tends to be efficiently transformed into NO_2 (Mazzeo et al., 2005). The higher O_3 level in the rural areas throughout the seasons indicated the role of oxidization during the transport. Flemming et al. (2005) also reported that the high O_3 levels in the rural area could be linked to the low level of NO emissions (e.g., the VOCs role; Ahrens, 2007). It is noted that seasonal O_3 concentrations in Jeju island (Jeju station; 33.51° N, 126.53° S) were higher than those found inland while the opposite situations were found for the other pollutants.

The seasonal CNSP pollutant concentrations were lower in summer due to heavy rainfall (despite high but intermittent photolysis rates) than in winter, when O_3 value was the lowest (Fig. 4 and Table 5). The maximum values of the CO, NO_2 and SO_2 were

CC BY

shown in the winter due to the low boundary layer height (e.g., Kaiser et al., 2007 for CO, NO_x) followed by the spring and the fall (see also Fig. 6c discussed later). Higher values of CO, NO_2 and PM_{10} over the SMA than in other regions were explained by the large population density and traffic emission, and industrial activity (Fig. 4). Higher NO_2 values in the SMA were also reported by Seo et al. (2014). The high SO_2 values over the coastal regions were due to the factories and power plants, and the high CO values inland were due to the active fossil fuel burning. Asian dust aerosol (e.g., PM_{10}) transported from China contributed to the spring peak in PM_{10}, and its spring maximum was due to the more intense solar radiation and lower amounts of precipitation than in other seasons (Table 5). These results suggest that the meteorological conditions were an important factor characterizing the seasonality of the air pollutants, while the emissions determined the levels of the pollutants.

Since the air pollution monitoring stations in South Korea are mostly located in the urban areas (Fig. 1), the spatial averages, which were arranged in a $0.1^\circ \times 0.1^\circ$ grid, indicated more urban characteristics than those in a $0.25^\circ \times 0.25^\circ$ grid (Table 5). The amounts of CNSP pollutants were larger in the former grid, while the O_3 values were larger in the latter. In particular, the annual value for NO_2 was remarkably greater by 16 % in the former than in the latter, suggesting that the vehicle emissions in the urban area were a primary source for that pollutant. On the other hand, the annual value for O_3 was smaller by 6 % in the $0.1^\circ \times 0.1^\circ$ grid than in the $0.25^\circ \times 0.25^\circ$ grid, implying that the O_3 levels in the suburban/rural/coastal areas were higher than in the urban ones (Fig. 4). These features were clear in the seasonal and annual values (Fig. 4 and Table 5).

4 Diurnal, weekly and annual variations of pollutants with land-use types

Figure 5 shows the spatial distributions of climatological annual averages in a $0.25^\circ \times 0.25^\circ$ grid over South Korea during 2002–2013 of the surface air pollutant observations for O_3 (ppb), CO (0.1 ppm), NO_2 (ppb), SO_2 (ppb) and PM_{10} (m^{-3}) in terms of the MEK

ACPD
15, 16985–17050, 2015

four land-use types of (a) residence, (b) commerce, (c) industry and (d) greenbelt. The distributions present unique characteristics by the four land-use types. For instance, Seoul, where both the residence and commerce types were dominant, was the most polluted with the CNSP pollutants in all of the land-use types. The CO was higher inland than in the coastal areas and the NO_2 was higher in the major cities including Seoul, Daegu, and Busan for all of the types. The distribution of SO_2 was similar to that of NO_2, but the former was larger in the coastal area than the latter due to its industry emissions. On the other hand, O_3 levels in the greenbelt type were the highest among the four types (Fig. 5d). Higher O_3 concentrations in the greenbelt areas occurred in spring due to the low NO share of the total NO_x and the intense solar radiation (Kuttler and Strassburger, 1999). The effect of solar radiation was larger in spring than in summer because of the East Asian summer monsoon (e.g., Park et al., 2015).

Figure 6 presents the (a) diurnal, (b) weekly and (c) annual variations in the spatial averages of Fig. 5 under the MEK four land-use types as follows; residence (black circle), commerce (blue cross), industry (red square), and greenbelt (green triangle). The diurnal variations of four kinds of pollutants were investigated in the previous studies by Flemming et al. (2005: for O_3, NO_2, SO_2, and PM_{10} in Germany) and Meng et al. (2009: for O_3, NO_x, SO_2, and CO in northern China). The former study also showed their weekly and annual variations over different air-quality regimes, while the latter emphasized significant seasonality in their diurnal cycles. In addition, Xu et al. (2008) investigated interannual variability of the surface O_3 in its diurnal cycle in four different seasons. In this study, the diurnal cycles of the five pollutants were analyzed for the different land-use regime. The results in the figure are also summarized in Tables 6 and 7. Table 6 shows the magnitude order of the five pollutant concentration averages of Fig. 6 in terms of the land-use types. The numbers in the table indicate the ranking of each pollutant based on the pollutant concentration values over the types. The greater concentration values corresponded to the upper ranking numbers. Only if the orders in the two types of grids were different from each other, then those in the parentheses were given for the $0.1^{\circ} \times 0.1^{\circ}$ grid. Table 7 also presents the spatial mean and standard

ACPD
15, 16985–17050, 2015

CC BY

deviation of the averages in a 0.25° × 0.25° grid. The values in parentheses in the table denote the mean and standard deviation in a 0.1° × 0.1° grid.

The typical shapes of the diurnal, weekly and annual cycles of the five pollutants were quite similar among the different land-use types but their magnitudes were systematically different depending on the types (Fig. 6 and Tables 6 and 7). In other words, the rank of the pollution level by the land-use type in the weekly and annual cycles was almost the same as in the diurnal cycle (Tables 6 and 7). In Table 6, the magnitude order (G > R > I > C) for O_3 with the types was exactly in the reverse order for NO_2 (C > I > R > G) for all cycles, suggesting the linkage between the two pollutants. The anti-correlations between the two pollutants in the diurnal cycle were also shown in Mazzeo et al. (2005) at a green city of Argentina and Han et al. (2011) in Tianjin, China. However, the reverse order for O_3 was different from those for SO_2 and PM_{10} (I > C > R > G). It is because SO_2 and PM_{10} pollutants were not uniquely associated with vehicle emissions (Flemming et al., 2005; see also Chen et al., 2001 for SO_2). The same order for the two pollutants with the land-use types suggested their emission sources from industrial activities rather than traffic emissions. It was interesting to note that the greenbelt area was commonly the lowest for the CNSP pollutants.

Since the primary production of O_3 was through photolysis, the O_3 started to rise in the morning and showed its peak at 4 p.m. before it rapidly decreased (Fig. 6a). The O_3 level was the highest in the greenbelt and the lowest in the commerce areas, while the levels of the O_3 for the residence and industry regimes were close to each other. The diurnal cycle of the O_3 in this study agreed with that of Flemming et al. (2005). Two peaks were shown in the diurnal cycle for CO, NO_2, and PM_{10}. The first peak was due to the increasing morning traffic and industrial activity (Kuttler and Strassburger, 1999, for the CO and PM_{10}). The second peak was due to the afternoon traffic and reduced boundary layer (Lee et al., 2014) during and after sunset. The daytime minima of these species were the results of the increased boundary layer height (Ulke and Mazzo, 1998; Lal et al., 2000; Han et al., 2011) as well as the oxidation processes for the chemically and photochemically reactive CO and NO_2 of which diurnal variations were generally

ACPD
15, 16985–17050, 2015

cc BY

out of phase with those of O_3 except for the midnight period (Kuttler and Strassburger, 1999; Lal et al., 2000). The diurnal cycle of the SO_2 in the commerce type also had two peaks similar to the other pollutants (CO, NO_2 and PM_{10}). The daytime minima could be explained by the high vertical mixing of their emissions (Meng et al., 2009). According to the diurnal variations of the CO and SO_2 over a suburban site in the USA, the patterns of their diurnal cycles were changed seasonally (Chen et al., 2001). The diurnal cycles of the O_3 and NO_2 without categorizing the land-use types were shown in Fig. 6a (O_3 and NO_2), consistent with those of Han et al. (2011) in Tianjin, China.

The commerce type in the daily, weekly, and annual cycles was ranked first for the CO and NO_2, but it was ranked second for the SO_2 and PM_{10} (Fig. 6 and Table 6). The industry type was ranked first for the SO_2 and PM_{10}, but it was ranked second for the NO_2. The residence type in a $0.25^\circ \times 0.25^\circ$ grid was ranked second with the industry regime for the CO, but it was ranked third for the NO_2, SO_2, and PM_{10}. These analyses indicated that the contribution of commerce was more important for the CO and NO_2, and that the contribution of the industry was more important for the SO_2 and PM_{10}. Since the commerce and industry types were associated with more vehicles and industrial activity, the CNSP pollutants in the residence type were lower than for these two types. Sharma et al. (2014) also reported that the PM_{10} levels in South Korea and abroad depended on different land-use types (urban, industry, rural/suburban).

The weekly cycles were analyzed for the different land-use types (Fig. 6b). The weekly cycle of the five pollutants was more remarkable in the land-use types with industrial and commercial activities, particularly in the industry type than in the green-belt one. The CO weekly cycle was pronounced in the commerce type as well as in the industry one. This implies that the MEK land-use types provided a reasonable discrimination between natural and anthropogenic pollutant sources. In general, on Sunday the level of the CNSP pollutants decreased but the O_3 values showed a peak. However, the degree of the Sunday pollutant values compared to those averaged for the working days from Tuesday to Friday (hereafter the working day average) varied by the pollutant species and land-use types. These Sunday low of the CNSP pollutants and

ACPD
15, 16985–17050, 2015

the Sunday high of O_3 (so-called the O_3 weekend effect; Larsen et al., 2003) were due to the anthropogenic activity that characterized the weekly emission pattern of South Korea.

Although the oxidization of chemicals during the transport (e.g., titration; Chen et al., 2002; Chou et al., 2006; Atkinson-Palombo et al., 2006) was in favor of O_3 production, the maximum O_3 in the greenbelt type suggested an important role of the volatile organic compounds emitted from vegetation (Fig. 6b for O_3), also discussed later in this study. In the figure, less O_3 reduction near anthropogenic sources (e.g., the commerce and residence areas) due to the decreased NO titration could induce an enhancement of O_3 particularly in the weekly cycle (e.g., Gilge et al., 2010). The NO_2 minimum on Sunday also occurred in Hohenpeissenberg, Germany due to less anthropogenic impact on weekends than on working days (Gilge et al., 2010). In Fig. 6b, the NO_2 minimum on Sunday (24 % reduction compared to the working day average) in the industry agreed with that of Beirle et al. (2003) over the industrialized regions (the USA, Europe and Japan) from the vertical column densities of tropospheric NO_2. The CO reduction on Sunday against the weekday average was the lowest (3–7 %) among the CNSP due to its longer life time (e.g., Gilge et al., 2010). The PM_{10} minimum on Sunday also occurred over a neighboring country, China (Choi et al., 2008). The O_3 Sunday maximum in the industry type was enhanced by ∼ 15 % with respect to the weekday average. The weekend effect of O_3 varied with the land-use types: I (15 %) > C (10 %) > R (9 %) > G (4 %). The increasing O_3 during the weekend could be associated with: (1) the decreasing NO_2 under the VOCs-limited regime, or (2) the behavior of the VOCs (e.g., Sakamoto el al., 2005), particularly the natural ones (or biogenic) in the greenbelt. Previous studies showed an increase in the O_3 and a decrease in the NO_2 during the weekends in the US and Germany (Flemming et al., 2005; Atkinson-Palombo et al., 2006). According to Gilge et al. (2010), anti-correlation between O_3 and NO_2 in their weekly cycles was less pronounced in summer due to photochemical O_3 production than in the other seasons.

ACPD
15, 16985–17050, 2015

CC BY

The annual cycle of O_3 generally showed a spring-early summer maximum and a wintertime minimum (Fig. 6c). This result was consistent with that of Pochanart et al. (1999) at Oki, Japan and on a regional scale in northeast Asia. The O_3 annual variation in the greenbelt presented primary and secondary peaks in May and October, respectively, reflecting seasonal changes of the photochemical intensity and Asian monsoon (Meng et al., 2009). However, the secondary peak was not clear in the other types (residence, commerce and industry). This suggested that the O_3 production in a monthly time-scale was sensitive to the local pollutant emissions with the land-use types. The NO_2 wintertime maxima could be associated with the fossil fuel consumption and photochemical oxidation of NO to NO_2 (Shon and Kim, 2011). The enhanced CO and NO_2 values in winter agreed with those of Gilge et al. (2010) over Hohenpeissenberg, Germany. Tropospheric NO_2 concentrations over South Korea also occurred in winter (at least 68 %) mainly due to local emissions (Mijling et al., 2013).

The SO_2 maximum in January in its annual cycle was generally similar to that of SO_2 emissions from China of Wang et al. (2013) (Fig. 6c). The values of the CNSP pollutants were lowest in June–August mainly due to the washout effect during the rainy period (e.g., Flemming et al., 2005; Meng et al., 2009; Yoo et al., 2014). Despite the low washout effect of CO, its reaction with HO radical was likely to be more important for the CO sink during the warm season (Stockwell and Calvert, 1983; Novelli et al., 2003; Gilge et al., 2010). The declining tendency of the SO_2 and NO_2 emissions in boreal summer also occurred in China because of the large-scale monsoon system (Wang et al., 2013). This implies that the NO_2 transport from China to South Korea could have more impact over the Korean Peninsula during wintertime dry season than during the summer and fall (Lee et al., 2014). The springtime PM_{10} maxima in its annual variations resulted from Asian Dust and meteorological conditions (Sharma et al., 2014).

Under the MEK four land-use types, the CNSP pollutants were overall larger in a $0.1^\circ \times 0.1^\circ$ grid (i.e., more urban characteristics), while the O_3 values were larger in a $0.25^\circ \times 0.25^\circ$ grid (i.e., more suburban/rural) (Table 8). In the annual average analyses, the $0.1^\circ \times 0.1^\circ$ grid averages (compared to those of the $0.25^\circ \times 0.25^\circ$ grid)

ACPD
15, 16985–17050, 2015

CC BY

generally tended to show the characteristics in large cities rather than in suburban areas or small cities, because the air-pollution monitoring stations were more densely located in the former areas, as mentioned earlier. The effects of the grid difference (i.e., the pollutant value in the 0.1° × 0.1° grid minus the value in the 0.25° × 0.25° grid) was quantitatively the greatest in the types of "commerce" for CO (+0.093 0.1 ppm), NO_2 (+2.969 ppb), PM_{10} (+0.711 $\mu g\,m^{-3}$), and O_3 (−0.735 ppb); and "industry" for SO_2 (+0.687 ppb) among the four land-use types. This result could be explained by the emissions of vehicle in the commerce type and the emissions of factories in the industry type.

5 Pollutant trends of O_3, NO_2, SO_2, CO, PM_{10}, and OX with respect to land-use types

Figure 7 shows the time series of the spatial averages of the monthly surface air pollutant anomalies for the five pollutant and OX concentrations in a 0.25° × 0.25° grid over South Korea during the period from January 2002 to December 2013 under the following MEK land-use types: residence (black solid), commerce (blue dashed), industry (red dotted), and greenbelt (green dashed). We calculated linear trends of the pollutant anomalies with respect to each of the land-use types. The ± trend values define the 95 % confidence intervals. Trend values of the pollutants are also summarized in Table 9, based on two types of analyses (the 0.1° × 0.1° and 0.25° × 0.25° grids) over the four land-use types of MEK of residence (R), commerce (C), industry (I), and greenbelt (G). The magnitude order for the trends of each of the pollutant over the types has been shown. It should be noted that the trend values were statistically significant except for a few of the NO_2 and SO_2 cases marked by an asterisk (*). Given the different spatiotemporal scales of the variability for the five pollutants (their scale order; CO > PM_{10} > O_3 > SO_2 > NO_x; Seinfeld and Pandis, 2006), the behavior of CO was likely to be related with the local, regional, and global effects but that of NO_2 with the local and regional ones (Gilge et al., 2010).

ACPD
15, 16985–17050, 2015

CC BY

The CNSP pollutants in South Korea tended to decrease regardless of the land-use types but interestingly the O_3 had an increasing tendency (Fig. 7 and Table 9). Since the five pollutants showed the same trends (either positive or negative) over all of the four types, the overall trends could reflect more the effects of regional emissions than local emissions. In the O_3 formation, for instance, the local part related with the level of primary pollutants (e.g., titration) while the regional part corresponded to the background O_3 concentration (Clapp and Jenkin, 2001). The regional background was likely to be large in the greenbelt area compared to the other land-use types in view of the reduced weekly cycle in the greenbelt (see also Fig. 6b). The declining trends of CNSP in a $0.25° \times 0.25°$ grid by the land-use type varied with the values of $-0.135 \sim -0.247$ ($0.1\,\mathrm{ppm\,yr^{-1}}$) for CO, $-0.042 \sim -0.295$ ($\mathrm{ppb\,yr^{-1}}$) for NO_2, $-0.036 \sim -0.140$ ($\mathrm{ppb\,yr^{-1}}$) for SO_2, and $-1.003 \sim -1.098$ ($\mathrm{\mu g\,m^{-3}\,yr^{-1}}$) for PM_{10}.

The downward trend of PM_{10} ($\sim 2\,\%\,\mathrm{yr^{-1}}$) in this study agreed with the result (0.4–2.7 $\%\,\mathrm{yr^{-1}}$) in Sharma et al. (2014) over major cities in the country during 1996–2010 (Fig. 7f and Table 9). The largest decrease for CO and SO_2 in the industry type was due to the reduced emissions from factories and power plants (Fig. 7d and e); the largest decrease for NO_2 in the residence type was associated with the reduced emission from vehicles (Fig. 7b); the commerce type was second (CO and SO_2) and third (PM_{10}); and the CNSP trends in the greenbelt type were low (third or fourth) except for PM_{10}. However, there was almost no difference in the PM_{10} declining trend between the land-use types. Kim and Shon (2011) reported that the sudden increase of PM_{10} in spring 2002 occurred due to the enhanced Asian Dust effect. The systematic decreasing trend of the CNSP pollutants suggested that the policy for air quality regulation worked successfully (Sharma et al., 2014 for PM_{10}).

In contrast to the CNSP case, it was interesting that the O_3 value in a $0.25° \times 0.25°$ grid increased with the rate of 0.352–0.501 ($\mathrm{ppb\,yr^{-1}}$; $\sim 1.6\,\%$) over the last 12 years although the CNSP pollutants were reduced (Fig. 7 and Table 9). This phenomenon was consistent with Mayer (1999), who reported that long-term trends of major air pollutants except for O_3 were decreasing, particularly in industrialized countries, but

ACPD
15, 16985–17050, 2015

CC BY

global O_3 levels were increasing during the early period of the twenty-first century (Cooper et al., 2010). Seo et al. (2014) reported an increase in the O_3 (+0.26 ppb yr^{-1}) in 46 cities in South Korea from 1999 to 2010. Also the O_3 increase (+0.48 ppb yr^{-1}) from 1990 to 2010, which was more consistent with our results, generally occurred for all of the seasons and day/night at most of the surface monitoring sites (Lee et al., 2014). This tendency was commonly shown in the two types of spatial grid analyses ($0.1^\circ \times 0.1^\circ$ and $0.25^\circ \times 0.25^\circ$ grid), possibly due to growing background O_3 (Table 9). The possibility of enhanced regional (background) O_3 as well as the local effect of the O_3 titration could be supported by the significant upward trends (0.205–0.396 ppb yr^{-1}; Table 9 and Fig. 7c) of the total oxidant (OX) despite the downward trends of the O_3 precursors (e.g., NO_2, CO, and PM_{10}). Specifically the significant positive trends of the OX values (0.26–0.300 ppb yr^{-1}) in the greenbelt type in the two kinds of grids ($0.1^\circ \times 0.1^\circ$, $0.25^\circ \times 0.25^\circ$) suggested the increase of background O_3 induced by its inflow from the regional scale, rather than the local scale. The upward trends of the OX in the both grids were commonly more pronounced in the commerce type than the other types, but the cause was unknown.

A positive trend of tropospheric ozone (3.1 % yr^{-1}) was clearly seen over Beijing from 2002–2010 in Wang et al. (2012), who emphasized a contribution in the downward O_3 flux from the stratosphere for the period. In spite of the CNSP decreasing trends in a $0.25^\circ \times 0.25^\circ$ grid (i.e., less urban features), the NO_2 tendency in a $0.1^\circ \times 0.1^\circ$ grid (i.e., more urban features) was not evident except for the residence (Table 9). Thus, the government regulation for NO_2 might not be very successful in large cities due to its diverse sources. Xu et al. (2008) suggested that the increased variability of the surface O_3 at a station in eastern China were mainly associated with the enhanced NO_x emission near the station.

The O_3 levels, which were related to the spatial variability in the local precursor emissions, were expected to vary with the land-use types. Seo et al. (2014) revealed that the long-term trends of the local precursor emissions on O_3 in South Korea could affect the O_3 trends locally, and in the country, significant enhancement of the background

ACPD
15, 16985–17050, 2015

CC BY

O_3 negatively affected the air quality. In order to understand the negative relationship in trend between O_3 and CNSP pollutants, particularly NO_2, we have investigated the relationship (i.e., correlation and weekly cycle) among O_3, NO_2 and VOCs with the land-use types further in Sects. 6 and 7. In this study, we focused on two issues: (1) which condition in view of the O_3 control in South Korea was more dominant, the VOCs-sensitivity or NO_2-sensitivity? (2) Did this condition significantly depend on the land-use types and the weekly cycles of the pollutants? The negative relationship between O_3 and NO_2 is expected in the VOCs-limited condition. Local effect of the pollutants compared to the regional (i.e., background) effect can be shown, based on their weekly variations at each station of the four land-use types.

6 Correlation between O_3 and NO_2 with land-use types

As shown in Fig. 7, the increasing O_3 trend was the opposite of the decreasing CNSP trends. The O_3 trends could be affected by interannual variations of the pollutant emissions (e.g., NO_x and VOCs) from their various sources and of the meteorological conditions (Kim et al., 2006). In view of the "O_3 control" strategy, the relationship between O_3 and NO_x (and the VOCs) was examined in many previous studies (e.g., Mazzeo et al., 2005; Han et al., 2011). There were various factors affecting the O_3: (1) local precursor emissions (e.g., NO_2, VOCs, and CO, etc.), (2) O_3 transport and its precursors from the local and remote sources; and (3) meteorological conditions (Seo et al., 2014). In this study we focused on the relationships on the local (grid) and regional (nationwide) scales in South Korea.

Figure 8 shows scatter diagrams of the O_3 vs. NO_2 from the monthly anomalies of Fig. 7 in South Korea under the four land-use types: (a) residence (black circle), (b) commerce (blue cross), (c) industry (red square) and (d) greenbelt (green triangle). The sample number in the monthly anomaly time series of each pollutant was 144 during 2002–2013. The temporal correlation coefficient (r) between the anomalies of the two pollutants was given together with the regression dotted line. The correlations

CC BY

in the residence and commerce types were statistically significant at a significance level of $p < 0.01$ (i.e., either $r > 0.194$ or $r < -0.194$). The correlation was also significant at $p < 0.05$ (i.e., either $r > 0.137$ or $r < -0.137$) in the industry type, but not significant in the greenbelt type due to the least NO_2 emissions. Therefore, these results indicated that the NO_2 emissions from vehicles in the residence and commerce areas were highly related to the O_3 change on the long-term time scale (Fig. 8a and b). Also the NO_2 probably affected the O_3 in the industry type. The above results agreed with those of Seo et al. (2014) who reported that the long-term O_3 variation over South Korea was similar to that of NO_2, but their trends were spatially different.

Figure 9 presents the relationship between O_3 and NO_2 in terms of the climatological annual averages over South Korea during 2002–2013 under the MEK four land-use types of: residence (R), commerce (C), industry (I), and greenbelt (G). The relationship was derived from the data all of the 283 stations, which were individually specified by one land-use type among the four types (Fig. 9a). Since the stations of residence were located nationwide (i.e., more than a half of all the stations), the relationship could be spatially different due to the population-related traffic emissions. Furthermore, the NO_2 decreasing trends in a $0.1^\circ \times 0.1^\circ$ grid (Table 9) were found significant only in the residence area, but not in the other types, despite the government control efforts (e.g., Shon and Kim, 2011). Note that the pollutant trends in a $0.25^\circ \times 0.25^\circ$ grid were given in Fig. 7, where the NO_2 trends were significant except for the commerce among the four land-use types. In order to further investigate the relationship within the residence areas based on the population size, we subdivided the locations of the 154 residence-type stations of Fig. 1a by the three regions (Fig. 9b) as follows: (i) the capital city of the country, Seoul (red circle), (ii) the SMA (green circle) except for Seoul, and (iii) outside of the SMA (blue circle). In this study, Seoul was defined as part of the SMA. The 20 and 50 % portions of the entire population in South Korea (∼ 50.5 million in 2014) lived in Seoul and the SMA, respectively. There were more traffic emissions in the SMA than outside of the SMA, particularly in the residence types.

ACPD
15, 16985–17050, 2015

CC BY

A very strong correlation ($p < 0.01$) of PM_{10} with the CO and NO_2 in their monthly dataset time series (Fig. 7) was likely to be associated with the traffic emission sources (see also Shon and Kim, 2011; Sharma et al., 2014). The correlations (0.42–0.56) in the residence and commerce were greater than those (0.32–0.47) in the greenbelt and industry, which was probably due to the vehicle emissions. In other words, more traffic emissions, which were related to the population density, were expected in Seoul than in the SMA excluding the capital city. The residence and commerce types were dominant in Seoul (Fig. 1a and b), while the residence and industry types predominantly existed in the SMA (Fig. 1b and d). Figure 9c is the same as Fig. 9a except for excluding the data in the SMA residence areas. Figure 9d is the same as Fig. 9a except for the O_3 and NO_2 relationships in the residence only over the three different regions shown in Fig. 9b. In Fig. 9d, the relationships over the three regions are shown in three colors, respectively.

The NO_2 (ppb) value was the highest in the commerce areas over South Korea (Fig. 9a and c; Table 10). The NO_2 concentration was estimated in the following order: commerce (C: 31.3) > Residence (R: 25.9) > Industry (I: 24.3) > Greenbelt (G: 13.3) (Fig. 9a). However, when the NO_2 (ppb) values in the region excluding the 74 SMA residence stations were examined, the order of the residence and industry areas was different from the previous case as follows: I (24.3) > R (20.3) (Fig. 9c). This result suggested that there were more NO_2-related traffic emissions (5.6 ppb) in the SMA residence areas than in the nationwide residence areas (Fig. 9a and c). The maxima (30.2 ppb) of the O_3 concentrations occurred in the greenbelt areas, while their minima were shown in the commerce areas (Fig. 9a and c). The order of magnitude of the O_3 was the opposite of that of the NO_2, showing an inverse relationship between the two pollutants (see also Han et al., 2011).

The traffic-induced pollutants were mainly NO, CO and PM_{10}, as well as VOCs, and the secondary trace gases of O_3 and NO_2 could be formed from these precursor substances during the photochemical reactions (Kuttler and Strassburger, 1999). They reported the inverse relationship of the O_3 vs. NO_2 within the urban areas (Essen,

ACPD
15, 16985–17050, 2015

CC BY

Germany) with the following five land-use types: motorway, the main and secondary roads, residence and greenbelt. The three types of the roads and motorway could correspond to the commerce areas in our study. Overall, our results were consistent with those of Kuttler and Strassburger (1999) who showed that the higher O_3 concentration was formed in urban green areas in the summer during intensive solar radiation, due to the relatively low share of NO in the total concentrations of NO_2 in the greenbelt areas. However, an inverse relationship has been also found in winter (Table 10). The consistency in the relationship of O_3 vs. NO_2 between the two studies supported the validation of the MEK classification method for the four land-use types. According to the monthly mean analysis of Xu et al. (2008) at a background station in eastern China, the negative correlation between O_3 and NO_x was found in the lowest 5 % of ozone in cold season than in the highest 5 % in warm season. Overall, the inverse relationship in Fig. 9a and c of this study, which systematically showed in the O_3 magnitude order ($G > R > I > C$; see also Table 6 in a $0.25^\circ \times 0.25^\circ$ grid) over the stations excluding the SMA residence areas in a non-grid, agreed well with the previous studies, suggesting that the four MEK land-use type classification was made reasonably.

As shown in Figs. 1a and 9a, the number of nationwide residence stations was the largest among the four land-use types. The spatial dependence of the O_3 vs. NO_2 relationship over the three different residence types (Fig. 9b; Seoul, the SMA except for Seoul, and outside of the SMA) where the amounts of traffic emissions were expected to be different due to the number density of automobiles per unit area (as shown in Fig. 1d) was interesting to note. Furthermore, relatively short-lived NO_2 compared to the other pollutants (CO, PM_{10}, O_3, and SO_2) in this study was used as a good indicator to reflect local and regional anthropogenic effects (Gilge et al., 2010). Although the SMA included Seoul, the residence region was separated into two sub-regions in this study in order to analyze the difference in the pollutants between them (Fig. 9d and Table 10). Heavier traffic generally occurred in Seoul than in the rest areas in the SMA. The NO_2 (ppb) concentrations in the residence areas over South Korea were estimated in the following order: Seoul (35.5 ± 2.53) > SMA except for Seoul (31.7 ± 4.03) > outside

ACPD
15, 16985–17050, 2015

cc BY

of the SMA (20.3 ± 4.94) (Fig. 9d). In the residence, there were pronounced reductions in the mean and standard deviation values of NO_2 due to the greater distance from the main traffic-induced pollution sources in the SMA including Seoul. The order of the O_3 (ppb) concentrations was the opposite of that for the NO_2 as follows; outside of the SMA (25.0 ± 4.03) > SMA except for Seoul (19.8 ± 1.74) > Seoul (18.6 ± 1.30). As a result, the MEK residence type, which had large variations in the two pollutant concentrations, could be required to be subdivided in the future in view of the O_3 vs. NO_2 relationship. However, the difference in the concentrations between the two regions within the SMA (i.e., Seoul and the SMA except for Seoul) was relatively small compared to that between the SMA and outside of the SMA, due to the their transport over the geographically neighboring locations.

7 Weekend effect of the O_3, NO_2, VOCs, OX, and VOC/NO_2 with land-use types

Since the O_3 formation at the surface can depend on two major precursors (i.e., NO_x and VOCs; Larsen et al., 2003) and the ratio of the NO_x and VOCs (e.g., Pudasainee et al., 2006), the relationship among these three pollutants (O_3, NO_2 and VOCs) was examined in the weekly cycles of many previous studies (e.g., Gilge et al., 2010 for O_3 and NO_2). The impact of the VOCs emission controls on the O_3 trend in northwest Europe was discussed in Derwent et al. (2003). Both the VOC emission data and the observations of atmospheric concentrations of VOCs in South Korea were lacking compared to those of the O_3 and NO_2, and, therefore, thus the VOC observational sites and records were sparse (as shown in Fig. 1e and Table 2). Figure 10 shows the weekly variations in the VOCs (green triangle), O_3 (red square) and NO_2 (blue rectangle) concentrations at 9 photochemical air pollution monitoring stations in South Korea since 2007 under the MEK four land-use types as follows: residence (R), commerce (C), industry (I), and greenbelt (G). The land-use types at the stations available for simultaneous observations (O_3, NO_2, and VOCs) were 4 residences (the sites of

ACPD
15, 16985–17050, 2015

cc BY

Bulgwang, Daemyoung, Gocheon and Goowol), 3 greenbelts (Seokmo, Taejong and Gwanin), a commerce area (Simgok) and an industry area (Joongheung).

The weekly cycle of the three pollutants was conspicuous in the residence and commerce areas (Fig. 10a–e). In the areas, the NO_2 and VOCs values were higher by 20–33 % on the weekdays than on the weekends due to variations in anthropogenic activity, while the O_3 value was higher by 17–21 % on the weekends. The VOCs increase on weekdays in the residence (Bulgwang) was probably due to vehicle emissions (e.g., Anthwal et al., 2010). The so-called weekend effect has been reported by Marr and Harley (2002a, b) and Fujita et al. (2003a, b) over the LA basin with higher O_3 concentrations on the weekends than on the weekdays. Marr and Harley (2002b) also found the weekly patterns of the lower NO_x and VOCs during weekend, out of phase with the higher O_3. Qin et al. (2004b) revealed that VOCs-limited condition for O_3 production and the NO_x-emission reduction in weekend could be associated with the weekend effect of O_3 in Southern California. In contrast to the residence and commerce areas, however, the weekly cycles of the three pollutants are not clear in the greenbelts and industry areas (Fig. 10f–i). In view of the negligible weekly cycle in the industry areas (Fig. 10f), the primary source for the cycle was traffic emission rather than the industrial factory activity. Since the industry station at Joongheung was located near the coast (Fig. 1e; red square), it could also have been influenced by meteorological factors (e.g., sea breeze). In addition, more observations for the industry and commerce types were required for detailed analysis, because the photochemical (VOCs) data in the two types were only available at a single station, respectively (Fig. 10e–f). In summary, more local effect influenced on the three pollutants in the residence and commerce areas, while regional (background) effect dominated in the greenbelt and industry areas.

It is interesting to note that the averages of the three pollutants at Simgok in the commerce (Fig. 10e) were highly contrast with those at Seokmo (Fig. 10g) in the greenbelt type. In other words, the O_3 level among the nine stations (Fig. 10) was the highest at Seokmo but relatively low at Simgok. However, the NO_2 and VOCs values had an opposite tendency with the O_3 case, showing their high values at the former (commerce)

ACPD
15, 16985–17050, 2015

site and their low values at the latter (greenbelt) site. According to the study of Seo et al. (2014), larger NO_x emissions over the metropolitan cities in the short-term and seasonality showed lower O_3 minima because of NO_x titration and a nocturnal NO_y chemical process. They also reported that the higher O_3 level near the Seokmo greenbelt (i.e., Ganghwa) were induced due to smaller NO_x emissions and the regional O_3 influxes from both the Yellow Sea (and China) and the SMA.

The decrease of local VOCs reduced O_3 with a reasonable amount of NO_2, and the ratio of VOCs to NO_x (i.e., VOC/NO_x) was an important factor for the O_3-control strategy (Marr and Harley, 2002a, b; Fujita et al., 2003a, b). Decreasing NO_x tended to increase O_3 formation when the VOC/NO_x ratio was less than the threshold values of 8–10 (Larsen et al., 2003). In addition, decreasing NO_x tended to decrease O_3 formation when the ratio was greater than the threshold values. In this study, the NO_2 value instead of NO_x was introduced for an approximate calculation of the ratio. The amounts of NO_2 approximately corresponded to 77–95 % of the amount of NO_x over a background station in northern China (Meng et al., 2009). Therefore, the ratios used in this study (i.e., VOC/NO_2) can be overestimated, compared to those of VOC/NO_x. The inter-relationship among the three pollutants was statistically examined in view of the individual role of NO_2 and VOCs for the O_3 control in this study. Figure 11 shows the scatter diagrams of the long-term averages of the (a) VOCs vs. NO_2, (b) O_3 vs. VOCs, (c) O_3 vs. NO_2, and (d) O_3 vs. VOC/NO_2 at the photochemical stations under the following four land-use types; residence (black circle), commerce (blue cross), industry (red square), and greenbelt (green triangle). The correlation coefficient and the dotted regression line were also given. The spatial coefficients were statistically significant for the cases of O_3 vs. NO_2 at $p < 0.01$ (i.e., $r < -0.750$; Fig. 11c) and for VOCs vs. NO_2 at $p < 0.05$ (i.e., $r > 0.583$; Fig. 11a). Meanwhile the correlations were not significant for the other two cases (O_3 vs. VOCs, and O_3 vs. VOC/NO_2) (Fig. 11b and d). The significant positive correlation between the VOCs and NO_2 might have been due to their common anthropogenic sources (e.g., transportation and industrial activities, etc.). Nine VOC values in Fig. 11a and b were systematically separated by their types in

ACPD
15, 16985–17050, 2015

view of magnitude. However, the residence values for the NO_2 and O_3 cases were not distinct from the industry case, due to their broad-range values in the residence areas (Fig. 11c). Overall, the pollutant values at the 4 residences and 3 greenbelts are systematically clustered in the 2-dimensional domains of Fig. 11, supporting the idea that the MEK land-use types are reasonable.

Figure 12 presents weekly variations of the OX and VOC/NO_2 values at each of the 9 photochemical stations of Fig. 10. The equally-weighted averages with respect to the four land-use types were also given for the OX and VOC/NO_2 in Fig. 12a and b (the grey cross dashed line), respectively. The weekend effect of OX in the residence and commerce was evident, while it was negligible in the greenbelt area (Fig. 12a). This contrast suggested the reduction of order of OX (ppb) is C (57.4) > R (53.6) > I (50.7) > G (45.4) (Table 11). The weak weekly cycle of OX in the greenbelt may be associated with the OX background level, although there was about a 9 ppb difference in OX between the greenbelt stations.

The average of VOC/NO_2 (the grey cross dashed line) did not show a clear weekly cycle (Fig. 12b). The weekly cycles of the ratio were almost negligible except for several stations. The industry type at Joongheung had a minimum on Tuesday in the weekly cycle, and its cause was unknown. Some weekend effects of the reduced ratio (i.e., the decrease on Saturday–Monday) at Daemyoung and Gocheon in the residence area occurred possibly due to the NO_2 reduction from less anthropogenic traffic emission. The ratio values tend to be relatively low in the greenbelt (2.–5.3) and residence (2.6–3.5) areas. The four type average was 6.6 (Table 11). Based on the average result at the photochemical stations, the VOCs-limited chemistry over South Korea was more common than the NO_x-limited one in the industry (Joongheung). As a result, except for the Joongheung station, the NO_2 decrease in weekend could result in the enhanced O_3 production at the other eight stations in South Korea. This phenomenon was more conspicuous in the residence and commerce areas (5 stations) due to the weekly cycle of anthropogenic vehicle emission than in the greenbelt areas (3 stations). The ratio result in this study over the SMA was consistent with that of Jin at al. (2012) who

ACPD
15, 16985–17050, 2015

CC BY

reported that the areas of the Seoul and Incheon cities were VOCs-limited using the Ozone Isopleth Plotting Package for Research (OZIPR) model. Also in the model study, 24 areas in Gyeonggi-do where approximately included the SMA except the two cities was equally either VOCs-limited or neutral. However the modelling had some limitations due to inaccuracy in emission inventories and transport.

Figure 13 and Table 11 summarized the long-term surface air pollutant averages (O_3, NO_2, OX, VOCs, and VOC/NO_2) at the 9 photochemical stations over South Korea since 2007 in terms of the four MEK land-use types. The values (O_3, NO_2, VOCs, and VOC/NO_2) in the bar graph in the figure were shown in the colors of orange, blue, grey and red, respectively. The OX values were given with the symbol "diamond" in green. The OX value, composed of NO_2-independent and NO_2-dependent parts, was utilized in order to understand the regional background O_3 concentration (i.e., the NO_2-independent one) (Mazzeo et al., 2005; Han et al., 2011). According to their studies, the OX values did not necessarily correlate to the levels of local primary pollution (i.e., NO_x-dependent). The residence values of the NO_2 and VOCs were 3–4 times greater than the greenbelt values. The NO_2 (ppb) concentrations in the four land-use types were estimated to be in the following order: commerce (C; 35.5) > Residence (R; 31.8) > Industry (I; 19.7) > Greenbelt (G; 9.9). The VOCs (ppbC) order was C (308.3) > I (199.6) > R (112.2) > G (31.2). Therefore, the anthropogenic sources of the VOC pollutants in the commerce and industry areas were likely to be more dominant than the natural ones. Nguyen et al. (2009) also reported the relative abundance of anthropogenic VOCs emissions compared to natural ones at a site in Seoul in 2004. The VOC order in the residence and commerce areas was different from NO_2 order, probably due to the different anthropogenic sources for the two different pollutants. On the other hand, the greenbelt and industry O_3 averages were greater than the residence and commerce ones by approximately 50 %. The order for O_3 (ppb) was G (35.3) > I (31.0) > C ≈ R (21.8–22.0), which was almost opposite to the NO_2 case.

ACPD
15, 16985–17050, 2015

cc BY

The ratio values of the VOC/NO_2 (3.6–8.7) in the residence, greenbelt, and commerce areas were generally smaller than the threshold values, while the ratio in the industry was the largest (10.2) of the four types (Table 11 and Fig. 13). The order for the ratio was I (10.2) > C (8.7) > G (3.9) > R (3.6). Therefore, the 8 stations except for the industry area among the 9 photochemical stations belonged to the VOCs-limited range which was defined as having the ratio value of less than 8 to 10 (see also Larsen et al., 2003). The industry station corresponded to the NO_x-limited chemistry. Higher O_3 levels on weekends (except in industry) could be associated with lower NO_2 values on weekends under the VOCs-limited O_3 formation regime. This tendency was also shown in the greenbelt as well as in the residence and commerce areas, although not as evident as the residence and commerce. This result was similar to the analysis of Marr and Harley (2002b) in California. They found that a shift in O_3 formation from NO_x-limited to VOCs-limited condition in the region could result from the reduction of VOCs more than that of NO_x. Based on the number of individual land-use type stations and their distribution over South Korea (Fig. 1), the VOCs control strategy for the O_3 reduction in this country was overall more effective than the NO_x control strategy. However, since the sample number of the photochemical stations in this study was limited particularly in the commerce and industry areas, the strategy could be shifted with the land-use types and more photochemical station data were needed for a more rigorous result. On the other hand, the VOCs-limited condition was also shown in Shanghai, China (Tie et al., 2013). On the other hand, according to the one-dimensional photochemical study of Liu et al. (2012) in Beijing, China, the reduction of either NO_2 or VOCs could induce the decrease of O_3 production in the transition regime from VOCs-limited to NO_x-limited, which was more pronounced in the layer of planetary boundary layer (PBL).

The OX values ranged from a minimum (45.4 ppb) in the greenbelt areas to a maximum (57.4 ppb) in the commerce area, indicating less variability than the other pollutant values (O_3, NO_2, and VOCs) (Fig. 13 and Table 11). This result agreed with the analysis of Mazzeo et al. (2005) at a green area of Argentina. The OX values in some areas

ACPD
15, 16985–17050, 2015

CC BY

in Taiwan were almost constant in previous studies (Chen et al., 2002; Chou et al., 2006). This result suggested that the "NO_x-titration" effect (e.g., Chou et al., 2006) was an important mechanism for the O_3 change. The temporal O_3 levels in the SMA and some inland areas were lower than those in the greenbelt and coastal areas due to NO_x titration effect (Kuttler and Strassburger, 1999; Ghim and Chang, 2002; Seo et al., 2014). The titration could have occurred locally even during nighttime without photochemistry from the nitrate formation and dry deposition by anthropogenic precursor emissions, and the higher O_3 values in the greenbelts related to the lower titration and the lower oxidization of NO (i.e., dilution) during the transport (Seo et al., 2014). Since local sources of both anthropogenic and biogenic hydrocarbons affected the oxidation (Kuttler and Strassburger, 1999; Clapp and Jenkin, 2001), their share needs to be further examined using, for instance, VOCs. Thus, O_3 formation in its weekly cycle could increase during weekend despite the reduced total (i.e., anthropogenic + natural) VOCs, because of their different species (Marr and Harley, 2002b).

8 Conclusions

We have comprehensively investigated the spatiotemporal variations in the surface air pollutants (O_3, NO_2, SO_2, CO, and PM_{10}) with the four land-use types of residence, commerce, industry and greenbelt over South Korea from 2002 to 2013, using routinely observed data at 283 stations. The spatiotemporal variations were analyzed in terms of the cycles (diurnal, weekly, and annual) of the pollutants, their trends and inter-relationship, based on the simultaneously observed hourly data. The VOCs data at 9 photochemical stations available since 2007 was also been utilized in order to examine their effects on the ozone chemistry. The pollutants, except for VOCs, were examined in the two spatial grids ($0.1^\circ \times 0.1^\circ$ and $0.25^\circ \times 0.25^\circ$) to present the pollutant difference between the urban and suburban cities.

The land-use types, set by the Korean government, were generally consistent with the satellite-derived land covers and with the previous result (Kuttler and Strassburger,

ACPD
15, 16985–17050, 2015

1999) of an anti-correlation between the O_3 and NO_2 in diverse city areas. The relationship between the two pollutants in the SMA residence areas was substantially different from that outside of the SMA, probably due to the local difference in the vehicle emissions. In addition, the pollutant values at the 4 residence and 3 greenbelts areas in this study were systematically clustered in the domains (O_3, NO_2, VOCs and VOC/NO_2), suggesting that the MEK land-use types were reasonable and objective.

The highest concentrations of air pollutants in the diurnal, weekly and annual cycles were found in the industrial areas for SO_2 and PM_{10}, in the commercial areas for NO_2 and CO and in the greenbelt areas for O_3, respectively. The CNSP pollutants, except for O_3, were generally higher in the big cities during the weekdays while the O_3 showed its highest values in the suburban areas or small cities during the weekends. The weekly cycle and trends of the O_3 were significantly out of phase with those of the NO_2, particularly in the residential and commercial areas, suggesting that vehicle emissions were a major source in those areas.

The values of the VOC/NO_2 ratio for each of land-use types turned out to be in the order of I (10.2) > C (8.7) > G (3.9) > R (3.6), which suggested that most of the areas (~ 70 %) in South Korea have to be under VOCs-limited sensitivities for ozone chemistry. In order to reduce O_3 in the substantial areas, it is more effective to decrease VOCs than NO_x in the short term. Regardless of the land-use types, the CNSP pollutants had significantly decreasing trends probably due to the effective government controls (Kim and Shon, 2011 for PM_{10}). As a result, the weekly cycles of the pollutants over South Korea were locally sensitive to the land-use types, while their long-term trends were most commonly similar to the types and regional areas. Total oxidant values (OX) with the land-use types were analyzed for the local and regional (or background) contributions of O_3, and the OX (ppb) order was C (57.4) > R (53.6) > I (50.7) > G (45.4). According to Seo et al. (2014), the elevated O_3 over South Korea (46 cities) in the short-term could be due to both local anthropogenic precursors (NO_x and VOCs, etc.) and their transport from China despite the O_3 uptrend

cc BY

($+0.5$–$2\,\%\,yr^{-1}$) in the Northern Hemisphere. In addition, the local wind could affect the ozone level over the SMA and Seoul (Ghim and Chang, 2000).

Complete observational datasets of the atmospheric composition (O_3, NO_x, CO, SO_2, PM_{10} and VOCs) from intensive field campaigns and their monitoring are required in the future together with their profile measurements for vertical mixing (e.g., Han et al., 2009) in order to reduce their pollution. In view of the O_3 control, the inter-relationships between the pollutants (O_3, NO_x, VOCs, PM_{10}, and CO) and their seasonal washout and vertical mixing have to be further investigated (e.g., Yoo et al., 2014 for washout). In addition, the O_3 level may increase with stronger insolation due to the reduced PM_{10} from environment regulation (e.g., Seo et al., 2014). The regional transport of the O_3 and NO_2 from China (Kim et al., 2012; Pochanart et al., 1999 for O_3 and CO), more accurate estimation and assessment on their emission inventories, and the meteorological and climatological effects (i.e., temperature, cloud and aerosol, air masses, etc.) on the pollutants are beyond the scope of this study, but they need to be studied in the future.

Acknowledgements. This study was supported by the National Research Foundation of Korea (NRF) grant funded by the Korean Government (MSIP) (no. 2009-0083527) and the Korean Ministry of Environment as the Eco-technopia 21 project (no. 201200016003).

References

Ahrens, C. D.: Meteorology Today; An Introduction to Weather, Climate, and the Environment, 8th edn., Thomson Brooks/Cole, Belmont, California, USA, 2007.

Anthwal, A., Park, C., Jung, K., Kim, M., and Kim, K.: The temporal and spatial distribution of volatile organic compounds (VOCs) in the urban residential atmosphere of Seoul, Korea, Asian J. Atmos. Environ., 4, 42–54, 2010.

Atkinson-Palombo, C. M., Miller, J. A., and Balling Jr., R. C.: Quantifying the ozone “weekend effect” at various locations in Phoenix, Arizona, Atmos. Environ., 40, 7644–7658, 2006.

ACPD

15, 16985–17050, 2015

Spatiotemporal variations of air pollutants with land-use types

J.-M. Yoo et al.

cc BY

Beirle, S., Platt, U., Wenig, M., and Wagner, T.: Weekly cycle of NO_2 by GOME measurements: a signature of anthropogenic sources, Atmos. Chem. Phys., 3, 2225–2232, doi:10.5194/acp-3-2225-2003, 2003.

Bian, H., Han, S., Tie, X., Sun, M., and Liu, A.: Evidence of impact of aerosols on surface ozone concentration in Tianjin, China, Atmos. Environ., 41, 4672–4681, 2007.

Brönnimann, S., Schuepbach, E., Zanis, P., Buchmann, B., and Wanner, H.: A climatology of regional background ozone at different elevations in Switzerland (1992–1998), Atmos. Environ., 34, 5191–5198, 2000.

Chen, C., Tsuang, B., Tu, C., Cheng, W., and Lin, M.: Wintertime vertical profiles of air pollutants over a suburban area in central Taiwan, Atmos. Environ., 36, 2049–2059, 2002.

Chen, L. W. A, Doddridge, B. G., Dickerson, R. R., Chow, J. C., Mueller, P. K., Quinn, J., and Butler, W. A.: Seasonal variations in elemental carbon aerosol, carbon monoxide and sulfur dioxide: implications for sources, Geophys. Res. Lett., 28, 1711–1714, 2001.

Choi, Y. S., Ho, C. H., Chen, D., Noh, Y. H., and Song, C. K.: Spectral analysis of weekly variation in PM_{10} mass concentration and meteorological conditions over China, Atmos. Environ., 42, 655–666, 2008.

Chou, C. C., Liu, S. C., Lin, C., Shiu, C., and Chang, K.: The trend of surface ozone in Taipei, Taiwan, and its causes: implications for ozone control strategies, Atmos. Environ., 40, 3898–3908, 2006.

Clapp, L. J. and Jenkin, M. E.: Analysis of the relationship between ambient levels of O_3, NO_2 and NO as a function of NO_x in the UK, Atmos. Environ., 35, 6391–6405, 2001.

Cooper, O., Parrish, D., Stohl, A., Trainer, M., Nédélec, P., Thouret, V., Cammas, J., Oltmans, S., Johnson, B., and Tarasick, D.: Increasing springtime ozone mixing ratios in the free troposphere over western North America, Nature, 463, 344–348, 2010.

De Fries, R., Hansen, M., Townshend, J., and Sohlberg, R.: Global land cover classifications at 8 km spatial resolution: the use of training data derived from Landsat imagery in decision tree classifiers, Int. J. Remote Sens., 19, 3141–3168, 1998.

Derwent, R., Jenkin, M., Saunders, S., Pilling, M., Simmonds, P., Passant, N., Dollard, G., Dumitrean, P., and Kent, A.: Photochemical ozone formation in north west Europe and its control, Atmos. Environ., 37, 1983–1991, 2003.

Diaz-de-Quijano, M., Penuelas, J., and Ribas, A.: Increasing interannual and altitudinal ozone mixing ratios in the Catalan Pyrenees, Atmos. Environ., 43, 6049–6057, doi:10.1016/j.atmosenv.2009.08.035, 2009.

ACPD
15, 16985–17050, 2015

Spatiotemporal variations of air pollutants with land-use types

J.-M. Yoo et al.

CC BY

Elbir, T., Kara, M., Bayram, A., Altiok, H., and Dumanoglu, Y.: Comparison of predicted and observed PM_{10} concentrations in several urban street canyons, Air Qual. Atmos. Health, 4, 121–131, doi:10.1007/s11869-010-0080-9, 2011.
Flemming, J., Stern, R., and Yamartino, R. J.: A new air quality regime classification scheme for O_3, NO_2, SO_2 and PM_{10} observations sites, Atmos. Environ., 39, 6121–6129, 2005.
Friedl, M. A., Sulla-Menashe, D., Tan, B., Schneider, A., Ramankutty, N., Sibley, A., and Huang, X.: MODIS Collection 5 global land cover: algorithm refinements and characterization of new datasets, Remote Sens. Environ., 114, 168–182, 2010.
Fujita, E. M., Campbell, D. E., Zielinska, B., Sagebiel, J. C., Bowen, J. L., Goliff, W. S., Stockwell, W. R., and Lawson, D. R.: Diurnal and weekday variations in the source contributions of ozone precursors in California's south coast air basin, J. Air Waste Manage., 53, 844–863, 2003a.
Fujita, E. M., Stockwell, W. R., Campbell, D. E., Keislar, R. E., and Lawson, D. R.: Evolution of the magnitude and spatial extent of the weekend ozone effect in California's south coast air basin, 1981–2000, J. Air Waste Manage., 53, 802–815, 2003b.
Ghim, Y. S. and Chang, Y.: Characteristics of ground-level ozone distributions in Korea for the period of 1990–1995, J. Geophys. Res.-Atmos., 105, 8877–8890, 2000.
Gilge, S., Plass-Duelmer, C., Fricke, W., Kaiser, A., Ries, L., Buchmann, B., and Steinbacher, M.: Ozone, carbon monoxide and nitrogen oxides time series at four alpine GAW mountain stations in central Europe, Atmos. Chem. Phys., 10, 12295–12316, doi:10.5194/acp-10-12295-2010, 2010.
Han, S., Bian, H., Tie, X., Xie, Y., Sun, M., and Liu, A.: Impact of nocturnal planetary boundary layer on urban air pollutants: measurements from a 250-m tower over Tianjin, China, J. Hazard. Mater., 162, 264–269, 2009.
Han, S., Bian, H., Feng, Y., Liu, A., Li, X., Zeng, F., and Zhang, X.: Analysis of the relationship between O_3, NO and NO_2 in Tianjin, China, Aerosol Air Qual. Res., 11, 128–139, 2011.
Hansen, M., DeFries, R., Townshend, J. R., and Sohlberg, R.: Global land cover classification at 1 km spatial resolution using a classification tree approach, Int. J. Remote Sens., 21, 1331–1364, 2000.
Jacobson, M. Z.: Atmospheric Pollution: History, Science, and Regulation, Cambridge University Press, Cambridge, UK, 2002.
Jin, L., Lee, S.-H., Shin, H.-J., and Kim, Y. P.: A Study on the Ozone Control Strategy using the OZIPR in the Seoul Metropolitan Area, Asian J. Atmos. Environ., 6, 111–117, 2012.

ACPD
15, 16985–17050, 2015

Kaiser, A., Scheifinger, H., Spangl, W., Weiss, A., Gilge, S., Fricke, W., Ries, L., Cemas, D., and Jesenovec, B.: Transport of nitrogen oxides, carbon monoxide and ozone to the alpine global atmosphere watch stations Jungfraujoch (Switzerland), Zugspitze and Hohenpeißenberg (Germany), Sonnblick (Austria) and Mt. Krvavec (Slovenia), Atmos. Environ., 41, 9273–9287, 2007.

Klemm, O., Stockwell, W. R., Schlager, H., and Krautstrunk, M.: NO_x or VOC limitation in East German ozone plumes?, J. Atmos. Chem., 25, 1–18, 2000.

Kim, J. Y., Kim, S., Ghim, Y. S., Song, C. H., and Yoon, S.: Aerosol properties at Gosan in Korea during two pollution episodes caused by contrasting weather conditions, Asia-Pac. J. Atmos. Sci., 48, 25–33, 2012.

Kim, K. and Shon, Z.: Long-term changes in PM_{10} levels in urban air in relation with air quality control efforts, Atmos. Environ., 45, 3309–3317, 2011.

Kim, N. K., Kim, Y. P., and Kang, C.-H.: Long-term trend of aerosol composition and direct radiative forcing due to aerosols over Gosan: TSP, PM_{10}, and $PM_{2.5}$ data between 1992 and 2008, Atmos. Environ., 45, 6107–6115, 2011.

Kim, N. K., Kim, Y. P., Morino, Y., Kurokawa, J., and Ohara, T.: Verification of NO_x emission inventory over South Korea using sectoral activity data and satellite observation of NO_2 vertical column densities, Atmos. Environ., 77, 496–508, 2013a.

Kim, S., Lee, M., Kim, S., Choi, S., Seok, S., and Kim, S.: Photochemical characteristics of high and low ozone episodes observed in the Taehwa Forest observatory (TFO) in June 2011 near Seoul South Korea, Asia-Pac. J. Atmos. Sci., 49, 325–331, 2013b.

Kim, S. W, Heckel, A., McKeen, S., Frost, G., Hsie, E., Trainer, M., Richter, A., Burrows, J., Peckham, S., and Grell, G.: Satellite-observed US power plant NO_x emission reductions and their impact on air quality, Geophys. Res. Lett., 33, L22812, doi:10.1029/2006GL027749, 2006.

Kuttler, W. and Strassburger, A.: Air quality measurements in urban green areas–a case study, Atmos. Environ., 33, 4101–4108, 1999.

Lal, S., Naja, M., and Subbaraya, B. H.: Seasonal variations in surface ozone and its precursors over an urban site in India, Atmos. Environ., 34, 2713–2724, 2000.

Lamsal, L., Martin, R., van Donkelaar, A., Celarier, E., Bucsela, E., Boersma, K., Dirksen, R., Luo, C., and Wang, Y.: Indirect validation of tropospheric nitrogen dioxide retrieved from the OMI satellite instrument: insight into the seasonal variation of nitrogen oxides at northern midlatitudes, J. Geophys. Res.-Atmos., 115, D05302, doi:10.1029/2009JD013351, 2010.

ACPD
15, 16985–17050, 2015

CC BY

Lamsal, L., Martin, R., Padmanabhan, A., van Donkelaar, A., Zhang, Q., Sioris, C., Chance, K., Kurosu, T., and Newchurch, M.: Application of satellite observations for timely updates to global anthropogenic NO_x emission inventories, Geophys. Res. Lett., 38, L05810, doi:10.1029/2010GL046476, 2011.

Larsen, L. C., Austin, J., Dolislager, L., Lashgari, A., McCauley, E., Motallebi, N., and Tran, H.: The Ozone Weekend Effect in California, California Environment of Protection Agency, Sacramento, California, USA, 2003.

Lee, H., Kim, S., Brioude, J., Cooper, O., Frost, G., Kim, C., Park, R., Trainer, M., and Woo, J.: Transport of NO_x in East Asia identified by satellite and in situ measurements and Lagrangian particle dispersion model simulations, J. Geophys. Res.-Atmos., 119, 2574–2596, doi:10.1002/2013JD021185, 2014.

Lee, Y.-R., Yoo, J.-M., Jeong, M.-J., Won, Y.-I., Hearty, T., and Shin, D.-B.: Comparison between MODIS and AIRS/AMSU satellite-derived surface skin temperatures, Atmos. Meas. Tech., 6, 445–455, doi:10.5194/amt-6-445-2013, 2013.

Liu, Z., Wang, Y., Gu, D., Zhao, C., Huey, L. G., Stickel, R., Liao, J., Shao, M., Zhu, T., Zeng, L., Amoroso, A., Costabile, F., Chang, C.-C., and Liu, S.-C.: Summertime photochemistry during CAREBeijing-2007: RO_x budgets and O_3 formation, Atmos. Chem. Phys., 12, 7737–7752, doi:10.5194/acp-12-7737-2012, 2012.

Marr, L. C. and Harley, R. A.: Modeling the effect of weekday-weekend differences in motor vehicle emissions on photochemical air pollution in central California, Environ. Sci. Technol., 36, 4099–4106, 2002a.

Marr, L. C. and Harley, R. A.: Spectral analysis of weekday–weekend differences in ambient ozone, nitrogen oxide, and non-methane hydrocarbon time series in California, Atmos. Environ., 36, 2327–2335, 2002b.

Masiol, M., Agostinelli, C., Formenton, G., Tarabotti, E., and Pavoni, B.: Thirteen years of air pollution hourly monitoring in a large city: potential sources, trends, cycles and effects of car-free days, Sci. Total Environ., 494–495, 84–96, doi:10.1016/j.scitotenv.2014.06.122, 2014.

Mayer, H.: Air pollution in cities, Atmos. Environ., 33, 4029–4037, 1999.

Mazzeo, N. A., Venegas, L. E., and Choren, H.: Analysis of NO, NO_2, O_3 and NO_x concentrations measured at a green area of Buenos Aires City during wintertime, Atmos. Environ., 39, 3055–3068, 2005.

ACPD
15, 16985–17050, 2015

CC BY

Meng, Z. Y., Xu, X. B., Yan, P., Ding, G. A., Tang, J., Lin, W. L., Xu, X. D., and Wang, S. F.: Characteristics of trace gaseous pollutants at a regional background station in Northern China, Atmos. Chem. Phys., 9, 927–936, doi:10.5194/acp-9-927-2009, 2009.

Mijling, B., van der A, R. J., and Zhang, Q.: Regional nitrogen oxides emission trends in East Asia observed from space, Atmos. Chem. Phys., 13, 12003–12012, doi:10.5194/acp-13-12003-2013, 2013.

Nevers, N. D.: Air Pollution Control Engineering, 2nd edn., McGraw-Hill Companies, Inc., New York, 571–573, 2000.

Nguyen, H. T., Kim, K., and Kim, M.: Volatile organic compounds at an urban monitoring station in Korea, J. Hazard. Mater., 161, 163–174, 2009.

Novelli, P. C., Masarie, K. A., Lang, P, M., Hall, B. D., Myers, R. C., and Elkins, J. W.: Reanalysis of tropospheric CO trends: effects of the 1997–1998 wildfires, J. Geophys. Res., 108, 4464, doi:10.1029/2002JD003031, 2003.

Oh, I., Kim, Y., and Kim, C.: An observational and numerical study of the effects of the late sea breeze on ozone distributions in the Busan metropolitan area, Korea, Atmos. Environ., 40, 1284–1298, 2006.

Pandey Deolal, S., Brunner, D., Steinbacher, M., Weers, U., and Staehelin, J.: Long-term in situ measurements of NO_x and NO_y at Jungfraujoch 1998–2009: time series analysis and evaluation, Atmos. Chem. Phys., 12, 2551–2566, doi:10.5194/acp-12-2551-2012, 2012.

Park, M. S., Lee, M. I., Kim, H. R., Im, J. H., and Yoo, J.-M.: Spatial and diurnal variations of storm heights in the East Asia summer monsoon: storm height regimes and large-scale diurnal modulation, Clim. Dynam., available online, 1432–0894, doi:10.1007/s00382-015-2610-5, 2015.

Pochanart, P., Hirokawa, J., Kajii, Y., Akimoto, H., and Nakao, M.: Influence of regional-scale anthropogenic activity in northeast Asia on seasonal variations of surface ozone and carbon monoxide observed at Oki, Japan, J. Geophys. Res.-Atmos., 104, 3621–3631, 1999.

Pudasainee, D., Sapkota, B., Shrestha, M. L., Kaga, A., Kondo, A., and Inoue, Y.: Ground level ozone concentrations and its association with NO_x and meteorological parameters in Kathmandu valley, Nepal, Atmos. Environ., 40, 8081–8087, 2006.

Qin, Y., Tonnesen, G., and Wang, Z.: One-hour and eight-hour average ozone in the California South Coast air quality management district: trends in peak values and sensitivity to precursors, Atmos. Environ., 38, 2197–2207, 2004a.

ACPD
15, 16985–17050, 2015

Spatiotemporal variations of air pollutants with land-use types

J.-M. Yoo et al.

Title Page
Abstract | Introduction
Conclusions | References
Tables | Figures
◀| |▶
◀ ▶
Back | Close
Full Screen / Esc
Printer-friendly Version
Interactive Discussion

CC BY

Qin, Y., Tonnesen, G., and Wang, Z.: Weekend/weekday differences of ozone, NO_x, CO, VOCs, PM_{10} and the light scatter during ozone season in southern California, Atmos. Environ., 38, 3069–3087, 2004b.
Sakamoto, M., Yoshimura, A., Kosaka, H., and Hiraki, T.: Study on weekend–weekday differences in ambient oxidant concentrations in Hyogo prefecture, J. Japan Soc. Atmos. Environ., 40, 201–208, 2005.
Seinfeld, J. H. and Pandis, S. N.: Atmosperic Chemistry and Physics – From Air Pollution to Climate Change, John Wiley & Sons, New Jersey, 2006.
Seo, J., Youn, D., Kim, J. Y., and Lee, H.: Extensive spatiotemporal analyses of surface ozone and related meteorological variables in South Korea for the period 1999–2010, Atmos. Chem. Phys., 14, 6395–6415, doi:10.5194/acp-14-6395-2014, 2014.
Sharma, A. P., Kim, K., Ahn, J., Shon, Z., Sohn, J., Lee, J., Ma, C., and Brown, R. J.: Ambient particulate matter (PM_{10}) concentrations in major urban areas of Korea during 1996–2010, Atmos. Pollut. Res., 5, 161–169, doi:10.5094/APR.2014.020, 2014.
Shon, Z. and Kim, K.: Impact of emission control strategy on NO_2 in urban areas of Korea, Atmos. Environ., 45, 808–812, 2011.
Stockwell, W. and Calvert, J. G.: The mechanism of the HO-SO_2 reaction, Atmos. Environ., 17, 2231–2235, 1983.
Tie, X., Geng, F., Guenther, A., Cao, J., Greenberg, J., Zhang, R., Apel, E., Li, G., Weinheimer, A., Chen, J., and Cai, C.: Megacity impacts on regional ozone formation: observations and WRF-Chem modeling for the MIRAGE-Shanghai field campaign, Atmos. Chem. Phys., 13, 5655–5669, doi:10.5194/acp-13-5655-2013, 2013.
Ulke, A. G. and Mazzeo, N. A.: Climatological aspects of the daytime mixing height in Buenos Aires city, Argentina, Atmos. Environ., 32, 1615–1622, 1998.
Valks, P., Pinardi, G., Richter, A., Lambert, J.-C., Hao, N., Loyola, D., Van Roozendael, M., and Emmadi, S.: Operational total and tropospheric NO_2 column retrieval for GOME-2, Atmos. Meas. Tech., 4, 1491–1514, doi:10.5194/amt-4-1491-2011, 2011.
Wang, T., Cheung, V. T., Anson, M., and Li, Y.: Ozone and related gaseous pollutants in the boundary layer of eastern China: overview of the recent measurements at a rural site, Geophys. Res. Lett., 28, 2373–2376, 2001.
Wang, W. X. and Wang, T.: On the origin and the trend of acid rain precipitation in China, Water Air Soil Poll., 85, 2295–2300, 1995.

CC BY

Wang, Y., McElroy, M. B., Munger, J. W., Hao, J., Ma, H., Nielsen, C. P., and Chen, Y.: Variations of O_3 and CO in summertime at a rural site near Beijing, Atmos. Chem. Phys., 8, 6355–6363, doi:10.5194/acp-8-6355-2008, 2008.
Wang, Y., Konopka, P., Liu, Y., Chen, H., Müller, R., Plöger, F., Riese, M., Cai, Z., and Lü, D.: Tropospheric ozone trend over Beijing from 2002–2010: ozonesonde measurements and modeling analysis, Atmos. Chem. Phys., 12, 8389–8399, doi:10.5194/acp-12-8389-2012, 2012.
Wang, Y., Zhang, Q. Q., He, K., Zhang, Q., and Chai, L.: Sulfate-nitrate-ammonium aerosols over China: response to 2000–2015 emission changes of sulfur dioxide, nitrogen oxides, and ammonia, Atmos. Chem. Phys., 13, 2635–2652, doi:10.5194/acp-13-2635-2013, 2013.
Wilks, D. S.: Statistical Methods in the Atmospheric Sciences, Academic Press, San Diego, California, USA, 1995.
WMO: WMO Global Atmosphere Watch (GAW) Strategic Plan (2008–2015), GAW Report No. 172 (WMO TD N O. 1384), World Meteorological Organization, Geneva, Switzerland, available at: http://gaw.empa.ch/gawsis (last access: 04 May 2015), 2007.
Xu, X., Lin, W., Wang, T., Yan, P., Tang, J., Meng, Z., and Wang, Y.: Long-term trend of surface ozone at a regional background station in eastern China 1991–2006: enhanced variability, Atmos. Chem. Phys., 8, 2595–2607, doi:10.5194/acp-8-2595-2008, 2008.
Yoo, J.-M., Lee, Y.-R., Kim, D.-C., Oh, S.-M., Jeong, M.-J., Stockwell, W., Kundu, P., Shin, D.-B., and Lee, S.-J.: New indices for wet scavenging of air pollutants (O_3, CO, NO_2, SO_2 and PM_{10}) by summertime rain, Atmos. Environ., 82, 226–237, 2014.
Zhang, Q., Streets, D. G., and He, K.: Satellite observations of recent power plant construction in Inner Mongolia, China, Geophys. Res. Lett., 36, L15809, doi:10.1029/2009GL038984, 2009.

ACPD
15, 16985–17050, 2015

Spatiotemporal variations of air pollutants with land-use types

J.-M. Yoo et al.

Title Page
Abstract | Introduction
Conclusions | References
Tables | Figures
◀◀ | ▶▶
◀ | ▶
Back | Close
Full Screen / Esc
Printer-friendly Version
Interactive Discussion

CC BY

Table 1. List of acronyms used in this study.

Acronyms	Original words	Details
R	Residence	Residential Areas: areas necessary to protect peaceful dwelling and sound living environment
C	Commerce	Commercial Areas: areas necessary to increase convenience in commerce and other businesses
I	Industry	Industrial Areas: areas necessary to increase convenience of industries
G	Greenbelt	Green Areas: areas requiring the conservation of green areas to protect the natural environment, farmland and forests, health and sanitation, security and to prevent any disorderly sprawl of cities
SMA	Seoul Metropolitan Area	
CNSP	CO, NO_2, SO_2 and PM_{10}	
OZIPR	Ozone Isopleth Plotting Package for Research	
MEK	Ministry of Environment of Korea	
MLIT	Ministry of Land, Infrastructure and Transport	
AVHRR	Advanced Very High Resolution Radiometer	
MODIS	Moderate-resolution Imaging Spectroradiometer	

ACPD
15, 16985–17050, 2015

Spatiotemporal variations of air pollutants with land-use types

J.-M. Yoo et al.

CC BY

ACPD
15, 16985–17050, 2015

Table 2. Data information of the surface air pollutants (O_3, CO, NO_2, SO_2 and PM_{10}) measured at 283 air pollution monitoring stations of the Ministry of Environment of Korea (MEK) in South Korea during 2002–2013. The information for the VOCs at 9 of the photochemical MEK stations, simultaneously measured with the other pollutants at the same sites, has also been shown. The 9 out of the total 19 VOCs stations were selected in this study, based on their locations and their relatively long-term records since 2007.

Air pollutant	Source	Period	Time interval	Number of stations Residence	Commerce	Industry	Greenbelt	Total
O_3, CO, NO_2, SO_2, PM_{10}	MEK	Jan 2002–Dec 2013	Hourly	154	57	35	37	283
VOCs	MEK	Jan 2007–Dec 2013	Hourly	3	1	0	3	7
VOCs at Daemyoung (128.57° E, 35.84° N)	MEK	Jan 2010–Dec 2013	Hourly	1	0	0	0	1
VOCs at Joongheung (126.68° E, 34.83° N)	MEK	Jan 2008–Dec 2013	Hourly	0	0	1	0	1

CC BY

Table 3. Methods and instruments for measuring the surface air pollutants (O_3, CO, NO_2, SO_2 and PM_{10}) at 283 MEK air pollution monitoring stations in South Korea during 2002–2013.

Air Pollutant	Method	Instrument
O_3	U.V Photometric Method	Thermo, 49i
CO	Non-Dispersive Infrared Method	Thermo, 48CTL
NO_2	Chemiluminescent Method	Thermo, 42CTL
SO_2	Pulse U.V Fluorescence Method	Thermo, 43CTL
PM_{10}	β-ray Absorption Method	Thermo, FH62-C14
VOC	TD-GC/MS (Thermal Desorption Gas Chromatography/Mass Spectrometry)	Agilent, Perkinelmer, Varian

ACPD
15, 16985–17050, 2015

Spatiotemporal variations of air pollutants with land-use types

J.-M. Yoo et al.

CC BY

Table 4. Comparison of the four land-use types of the MEK (residence, commerce, industry, and greenbelt) for 283 air pollution monitoring stations of the MEK during 2002–2012 with the satellite-derived land-cover types of the AVHRR and MODIS in a $0.25^{\circ} \times 0.25^{\circ}$ grid. The AVHRR data were available for 13 land-cover types over the globe at a 1 km × 1 km pixel resolution during 1981–1994 (e.g., De Fries et al., 1998; Hansen et al., 2000). The MODIS data have been derived for 17 land-cover types over the globe at a 5 km × 5 km spatial resolution during 2002–2012 (e.g., Friedl et al., 2010). In this study, for comparison, the AVHRR and MODIS original types were regrouped into the following four land-cover types: forest/wood, grass/shrub, urban/built-up and water. In the table, the values with and without parentheses indicate the MODIS and AVHRR data, respectively.

Land Cover	Residence (%)	Commerce (%)	Industry (%)	Greenbelt (%)
Forest/Wood	12.4 (31.8)	15.8 (35.8)	8.6 (26.2)	35.2 (37.2)
Grass/Shrub	58.4 (27.5)	43.9 (18.0)	60.0 (19.2)	43.2 (21.8)
Urban/Built-up	19.5 (28.8)	33.3 (32.2)	11.4 (28.6)	0.0 (16.4)
Water	9.7 (11.9)	7.0 (14.0)	20.0 (26.0)	21.6 (24.6)

ACPD
15, 16985–17050, 2015

Table 5. Climatological averages of (a) O_3 (ppb), (b) CO (0.1 ppm), (c) NO_2 (ppb), (d) SO_2 (ppb), and (e) PM_{10} (µ gm^{-3}) in two types of spatial grids (0.25° × 0.25° and 0.1° × 0.1°) over South Korea during 2002–2013. The standard deviation (σ) values of the five kinds of variables are also presented with the ± values.

	Spring	Summer	Fall	Winter	Annual
⟨0.25° × 0.25°⟩					
O_3 (ppb yr^{-1})	34.93 ± 7.69	27.22 ± 4.44	22.34 ± 7.22	19.62 ± 7.08	26.08 ± 6.33
CO (0.1 ppm yr^{-1})	5.38 ± 1.12	4.16 ± 0.92	5.41 ± 1.24	7.23 ± 2.05	5.53 ± 1.23
NO_2 (ppb yr^{-1})	18.10 ± 8.25	13.14 ± 6.25	17.92 ± 8.35	21.13 ± 9.01	17.54 ± 7.88
SO_2 (ppb yr^{-1})	4.89 ± 1.65	3.57 ± 1.71	4.23 ± 1.61	6.49 ± 2.43	4.78 ± 1.67
PM_{10} (µg m^{-3} yr^{-1})	64.47 ± 8.41	41.2 ± 6.21	45.57 ± 7.49	54.82 ± 10.89	51.46 ± 7.72
⟨0.1° × 0.1°⟩					
O_3 (ppb yr^{-1})	33.08 ± 7.37	26.42 ± 4.24	20.87 ± 6.51	17.95 ± 6.59	24.63 ± 5.88
CO (0.1 ppm yr^{-1})	5.38 ± 1.14	4.21 ± 0.97	5.49 ± 1.30	7.30 ± 2.06	5.58 ± 1.27
NO_2 (ppb yr^{-1})	21.10 ± 9.59	15.48 ± 7.42	20.79 ± 9.27	24.12 ± 9.99	20.34 ± 8.96
SO_2 (ppb yr^{-1})	5.27 ± 1.97	3.97 ± 2.10	4.60 ± 1.86	6.82 ± 2.45	5.15 ± 1.90
PM_{10} (µg m^{-3} yr^{-1})	66.53 ± 9.90	42.91 ± 7.01	47.63 ± 8.53	57.31 ± 12.30	53.58 ± 8.91

ACPD
15, 16985–17050, 2015

CC BY

Table 6. The magnitude order of the surface air pollutant concentration averages (O_3, CO, NO_2, SO_2, and PM_{10}) in the diurnal, weekly and annual variations of Fig. 6 over South Korea during 2002–2013 in a 0.25° × 0.25° grid in terms of the four land-use types of MEK as follows: residence (R), commerce (C), industry (I) and greenbelt (G). The numbers in the table indicate the ranking of each pollutant, based on the pollutant concentration values over the types. Here the greater concentration, the higher ranking. If the orders in the two grids are different from each other, then those in parentheses have been shown for the 0.1° × 0.1° grid.

Cycle and pollutants	Residence		Commerce		Industry		Greenbelt	
Diurnal								
O_3	24.3 ± 8.07	(23.5 ± 8.19)	21.3 ± 6.93	(20.2 ± 6.80)	23.5 ± 7.24	(23.5 ± 7.20)	30.9 ± 7.69	(30.4 ± 7.78)
CO	5.7 ± 0.56	(5.7 ± 0.60)	6.2 ± 0.63	(6.4 ± 0.60)	5.7 ± 0.39	(5.8 ± 0.42)	4.6 ± 0.26	(4.7 ± 0.28)
NO_2	21.1 ± 3.62	(23.1 ± 3.87)	25.1 ± 4.19	(28.1 ± 4.33)	23.2 ± 3.02	(23.8 ± 2.98)	11.7 ± 1.52	(12.7 ± 1.70)
SO_2	5.2 ± 0.33	(5.3 ± 0.35)	5.6 ± 0.39	(5.7 ± 0.41)	6.8 ± 0.79	(7.5 ± 0.85)	3.3 ± 0.23	(3.4 ± 0.24)
PM_{10}	52.7 ± 3.04	(53.3 ± 2.87)	54. ± 3.37	(55.2 ± 3.28)	56. ± 2.98	(56.4 ± 3.01)	48.4 ± 2.20	(49.5 ± 2.33)
Weekly								
O_3	24.2 ± 0.72	(23.4 ± 0.81)	21.2 ± 0.75	(20.2 ± 0.84)	23.4 ± 1.19	(23.4 ± 1.22)	30.8 ± 0.41	(30.3 ± 0.46)
CO	5.7 ± 0.01	(5.7 ± 0.11)	6.2 ± 0.16	(6.4 ± 0.18)	5.7 ± 0.14	(5.8 ± 0.14)	4.6 ± 0.01	(4.7 ± 0.01)
NO_2	21.1 ± 1.32	(23.1 ± 1.48)	25.1 ± 1.42	(28.2 ± 1.65)	23.2 ± 1.99	(23.8 ± 2.03)	11.7 ± 0.69	(12.7 ± 0.78)
SO_2	5.2 ± 0.15	(5.3 ± 0.15)	5.5 ± 0.12	(5.7 ± 0.15)	6.8 ± 0.29	(7.5 ± 0.30)	3.3 ± 0.02	(3.4 ± 0.01)
PM_{10}	52.7 ± 1.19	(53.3 ± 1.31)	54. ± 1.20	(55.2 ± 1.43)	56.1 ± 2.25	(56.4 ± 2.25)	48.4 ± 0.71	(49.4 ± 0.82)
Annual								
O_3	24. ± 6.96	(23.4 ± 6.89)	20.9 ± 6.25	(20.2 ± 6.12)	23.2 ± 6.23	(23.4 ± 6.28)	30.7 ± 7.35	(30.3 ± 7.34)
CO	5.8 ± 1.32	(5.7 ± 1.30)	6.3 ± 1.42	(6.4 ± 1.36)	5.8 ± 0.93	(5.8 ± 0.93)	4.7 ± 0.89	(4.7 ± 0.92)
NO_2	21.1 ± 4.01	(23.2 ± 4.27)	25.2 ± 3.79	(28.2 ± 3.91)	23.2 ± 3.47	(23.8 ± 3.55)	11.7 ± 2.37	(12.8 ± 2.59)
SO_2	5.2 ± 1.28	(5.3 ± 1.23)	5.6 ± 1.39	(5.7 ± 1.31)	6.8 ± 0.87	(7.5 ± 0.76)	3.4 ± 0.92	(3.4 ± 0.93)
PM_{10}	53.1 ± 10.40	(53.3 ± 10.45)	54.5 ± 10.93	(55.2 ± 10.83)	56.4 ± 9.68	(56.3 ± 9.45)	48.8 ± 9.85	(49.6 ± 9.82)

ACPD
15, 16985–17050, 2015

CC BY

Table 7. The spatial mean and standard deviation of the surface air pollutant concentration averages (O_3, CO, NO_2, SO_2, and PM_{10}) in the diurnal, weekly, and annual variations over South Korea during 2002–2013 in a 0.25° × 0.25° grid in terms of the four land-use types of MEK as follows: residence (R), commerce (C), industry (I), and greenbelt (G). Here the values in parentheses denote the mean and standard deviation in a 0.1° × 0.1° grid.

Cycle/pollutants	Residence	Commerce	Industry	Greenbelt	Order
Diurnal					
O_3	2 (2)	4 (4)	3 (3)	1 (1)	G > R > I > C
CO	2 (3)	1 (1)	3 (2)	4 (4)	C > R > I > G (C > I > R > G)
NO_2	3 (3)	1 (1)	2 (2)	4 (4)	C > I > R > G
SO_2	3 (3)	2 (2)	1 (1)	4 (4)	I > C > R > G
PM_{10}	3 (3)	2 (2)	1 (1)	4 (4)	I > C > R > G
Weekly					
O_3	2 (2)	4 (4)	3 (3)	1 (1)	G > R > I > C
CO	2 (3)	1 (1)	3 (2)	4 (4)	C > R > I > G (C > I > R > G)
NO_2	3 (3)	1 (1)	2 (2)	4 (4)	C > I > R > G
SO_2	3 (3)	2 (2)	1 (1)	4 (4)	I > C > R > G
PM_{10}	3 (3)	2 (2)	1 (1)	4 (4)	I > C > R > G
Annual					
O_3	2 (2)	4 (4)	3 (3)	1 (1)	G > R > I > C
CO	2 (3)	1 (1)	3 (2)	4 (4)	C > R > I > G (C > I > R > G)
NO_2	3 (3)	1 (1)	2 (2)	4 (4)	C > I > R > G
SO_2	3 (3)	2 (2)	1 (1)	4 (4)	I > C > R > G
PM_{10}	3 (3)	2 (2)	1 (1)	4 (4)	I > C > R > G

ACPD
15, 16985–17050, 2015

Spatiotemporal variations of air pollutants with land-use types

J.-M. Yoo et al.

Table 8. Comparisons of the climatological annual averages over South Korea during 2002–2013, based on the two types of spatial scale analyses of the $0.1^{\circ} \times 0.1^{\circ}$ and $0.25^{\circ} \times 0.25^{\circ}$ grids. The $0.1^{\circ} \times 0.1^{\circ}$ grid averages (compared to those of $0.25^{\circ} \times 0.25^{\circ}$) generally tend to show the characteristics in big urban cities rather than in suburban small suburban cities, because the air-pollution monitoring stations are more densely located in the former areas.

Air pollutant	Average ($0.1^{\circ} \times 0.1^{\circ}$) minus Average ($0.25^{\circ} \times 0.25^{\circ}$)			
	Residence	Commerce	Industry	Greenbelt
O_3 (ppb)	−0.513	−0.735	0.181	−0.342
CO (ppb)	−0.067	0.093	0.052	0.009
NO_2 (ppb)	2.020	2.969	0.573	0.767
SO_2 (ppb)	0.036	0.123	0.687	0.033
PM_{10} ($\mu g\,m^{-3}$)	0.270	0.711	−0.012	0.409

Discussion Paper | Discussion Paper | Discussion Paper | Discussion Paper |

ACPD
15, 16985–17050, 2015

CC BY

Table 9. Trends of surface air pollutants (O_3, NO_2, OX, CO, SO_2 and PM_{10}) over South Korea during 2002–2013, based on the three types of analyses ($0.1^{\circ} \times 0.1^{\circ}$ grid and $0.25^{\circ} \times 0.25^{\circ}$ grid) over the four land-use types of the MEK of residence (R), commerce (C), industry (I), and greenbelt (G). The magnitude order for the trends of each of the pollutant over the types has been shown in the figures. The ± trend values indicate the 95 % confidence intervals. It should be noted that the trend values are statistically significant except for some of the NO_2 and SO_2 cases, marked by an asterisk (*).

	Residence	Commerce	Industry	Greenbelt	Trend	Order
$0.25^{\circ} \times 0.25^{\circ}$						
O_3 (ppb yr^{-1})	0.501 ± 0.098	0.407 ± 0.095	0.352 ± 0.093	0.369 ± 0.094	increase	R > C > G > I
NO_2 (ppb yr^{-1})	−0.295 ± 0.081	−0.042 ± 0.088*	−0.135 ± 0.084	−0.100 ± 0.053	decrease	R > I > G > C*
OX (ppb yr^{-1})	0.205 ± 0.107	0.365 ± 0.103	0.231 ± 0.113	0.260 ± 0.103	increase	C > G > I > R
CO (0.1 ppm yr^{-1})	−0.202 ± 0.021	−0.210 ± 0.021	−0.247 ± 0.025	−0.135 ± 0.022	decrease	I > C > R > G
SO_2 (ppb yr^{-1})	−0.036 ± 0.024	−0.114 ± 0.028	−0.140 ± 0.029	−0.060 ± 0.016	decrease	I > C > G > R
PM_{10} (µg m^{-3} yr^{-1})	−1.038 ± 0.459	−1.014 ± 0.456	−1.003 ± 0.480	−1.098 ± 0.485	decrease	G > R > C > I
$0.1^{\circ} \times 0.1^{\circ}$						
O_3 (ppb yr^{-1})	0.545 ± 0.096	0.462 ± 0.092	0.340 ± 0.094	0.326 ± 0.095	increase	R > C > I > G
NO_2 (ppb yr^{-1})	−0.240 ± 0.083	−0.078 ± 0.092*	−0.054 ± 0.084*	−0.023 ± 0.054*	decrease	R > C* > I* > G*
OX (ppb yr^{-1})	0.304 ± 0.108	0.396 ± 0.106	0.299 ± 0.110	0.300 ± 0.102	increase	C > R > G > I
CO (0.1 ppm yr^{-1})	−0.175 ± 0.021	−0.204 ± 0.020	−0.246 ± 0.025	−0.124 ± 0.022	decrease	I > C > R > G
SO_2 (ppb yr^{-1})	−0.019 ± 0.023*	−0.104 ± 0.027	−0.177 ± 0.030	−0.050 ± 0.015	decrease	I > C > G > R
PM_{10} (µg m^{-3} yr^{-1})	−1.374 ± 0.535	−1.290 ± 0.474	−0.926 ± 0.492	−1.049 ± 0.485	decrease	R > C > G > I

ACPD
15, 16985–17050, 2015

Spatiotemporal variations of air pollutants with land-use types

J.-M. Yoo et al.

cc BY

Table 10. Climatological average value of O_3 (ppb) and NO_2 (ppb) over South Korea during 2002–2013 in terms of the MEK four land-use types (residence, commerce, industry and greenbelt) over the 283 total stations and the 209 stations excluding the 74 SMA residence areas, respectively. The spatial variation in the pollutant concentrations for the individual type is presented with the standard deviation of ± values. The number in the parenthesis indicates the ranking of each pollutant, based on concentration value over the type.

Land-use type	All stations O_3	All stations NO_2	Stations excluding the SMA residence areas O_3	Stations excluding the SMA residence areas NO_2
⟨Annual⟩				
Residence	22.4 ± 4.32 (3)	25.9 ± 8.15 (2)	25.0 ± 4.03 (2)	20.3 ± 4.94 (3)
Commerce	19.2 ± 4.85 (4)	31.3 ± 12.00 (1)		
Industry	23.4 ± 4.32 (2)	24.3 ± 6.89 (3)	23.4 ± 4.32 (3)	24.3 ± 6.89 (2)
Greenbelt	30.2 ± 7.83 (1)	13.3 ± 9.63 (4)		
⟨Winter only⟩				
Residence	15.4 ± 4.91 (3)	30.6 ± 9.04 (2)	18.3 ± 4.80 (2)	24.4 ± 6.0 (3)
Commerce	13.2 ± 4.28 (4)	34.6 ± 11.29 (1)		
Industry	16.7 ± 4.43 (2)	27.8 ± 7.52 (3)	16.7 ± 4.43 (3)	27.8 ± 7.52 (2)
Greenbelt	24.4 ± 8.72 (1)	16.3 ± 11.27 (4)		

ACPD
15, 16985–17050, 2015

Table 11. The spatial mean values of the long-term surface air pollutant concentration averages (O_3, NO_2, OX, VOC, and VOC/NO_2) at 9 of the photochemical air pollution monitoring stations of the MEK over South Korea since 2007 in terms of the four MEK land-use categories as follows: residence (R), commerce (C), industry (I), and greenbelt (G).

Air pollutant	Residence	Commerce	Industry	Greenbelt	Average
O_3 (ppb)	21.8 ± 1.24	22.0	31.0	35.5 ± 0.43	27.6
NO_2 (ppb)	31.8 ± 2.18	35.5	19.7	9.9 ± 0.39	24.2
$OX = O_3 + NO_2$ (ppb)	53.6 ± 1.00	57.4	50.7	45.4 ± 0.29	51.8
VOC (ppbC)	112.2 ± 14.84	308.3	199.6	31.2 ± 2.14	162.8
VOC/NO_2	3.6 ± 0.27	8.7	10.2	3.9 ± 0.13	6.6

ACPD
15, 16985–17050, 2015

Spatiotemporal variations of air pollutants with land-use types

J.-M. Yoo et al.

CC BY

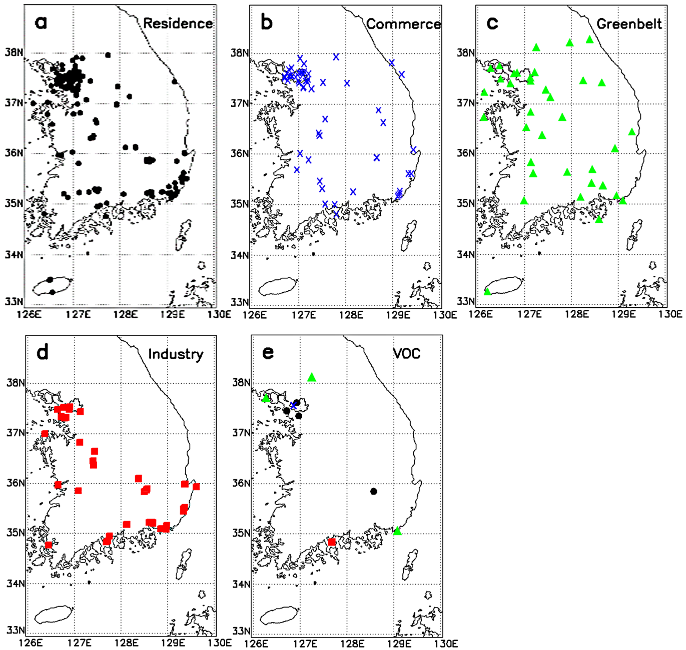

Figure 1. Locations of surface air pollution (O_3, CO, NO_2, SO_2, and PM_{10}) monitoring stations in South Korea during 2002–2013 under the MEK four land-use types of **(a)** residence (black circle), **(b)** commerce (blue cross), **(c)** greenbelt (green triangle) and **(d)** industry (red square). **(e)** Locations of the VOC monitoring stations, used in this study, under the four land-use types. The VOCs and the five kinds of air pollutants were simultaneously measured at the nine stations in Fig. 1e. Please see Table 1 for the observational periods of VOCs.

ACPD
15, 16985–17050, 2015

Spatiotemporal variations of air pollutants with land-use types

J.-M. Yoo et al.

cc BY

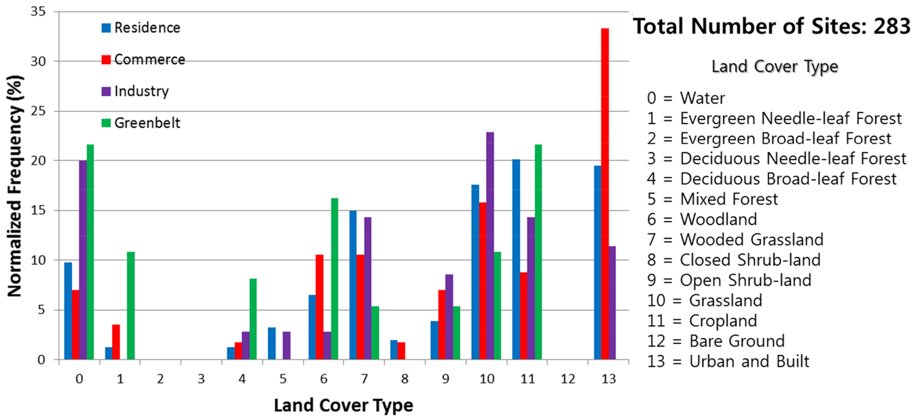

Figure 2. Satellite-derived AVHRR land-cover types with respect to the MEK four land-use types (residence, commerce, industry and greenbelt) of 283 air pollution monitoring stations of the MEK in South Korea. The 13 AVHRR types were given at a 1 km × 1 km pixel resolution (e.g., De Fries et al., 1998; Hansen et al., 2000).

ACPD
15, 16985–17050, 2015

CC BY

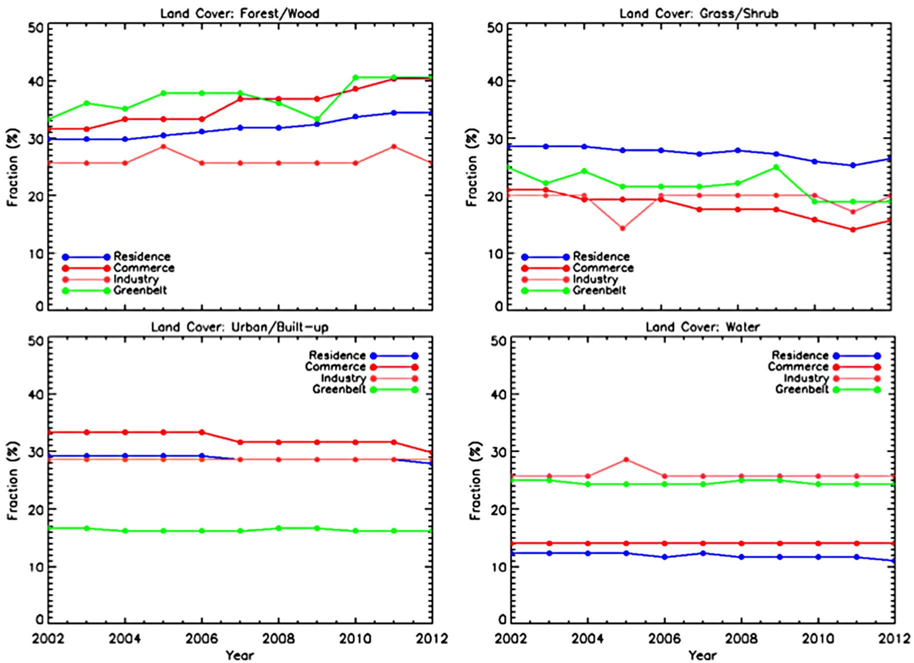

Figure 3. Interannual variations of the satellite-derived MODIS land-cover types (%) vs. the MEK four land-use types (residence, commerce, industry and greenbelt) of the 283 air pollution monitoring stations in South Korea during 2002–2012. In this study, for ease of comparison, the MODIS original types were regrouped into the following four covers; forest/wood, green/shrub, urban/built-up and water.

CC BY

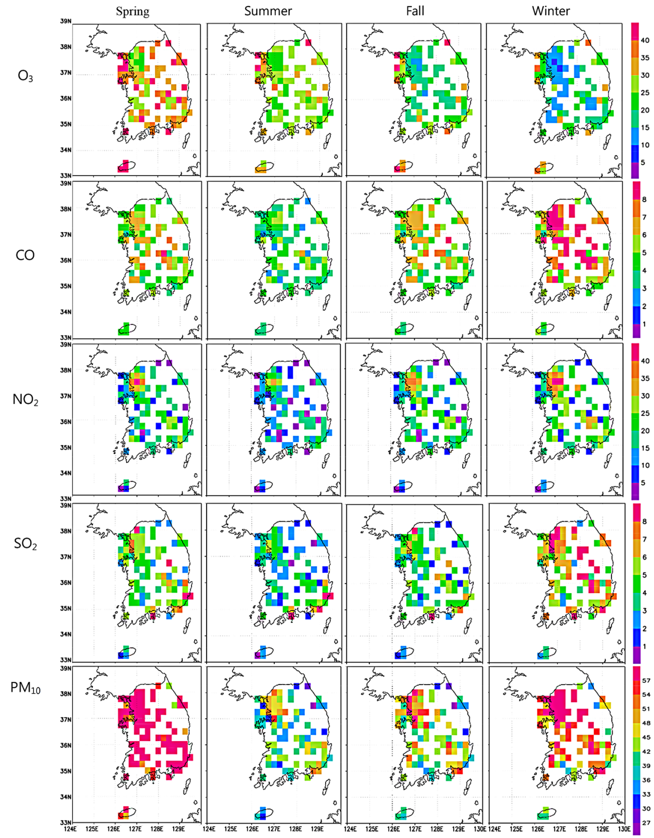

Figure 4. Climatological seasonal averages of O_3 (ppb), CO (0.1 ppm), SO_2 (ppb), NO_2 (ppb), and PM_{10} ($\mu g\,m^{-3}$) in a 0.25° × 0.25° grid over South Korea during 2002–2013.

ACPD
15, 16985–17050, 2015

CC BY

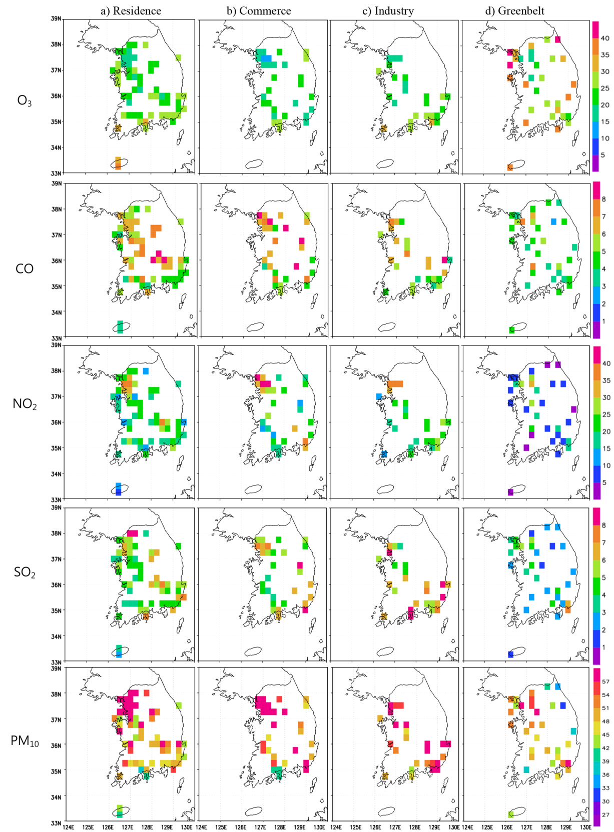

Figure 5. Climatological annual averages in a 0.25° × 0.25° grid over South Korea during 2002–2013 of the surface air pollutant observations of O_3 (ppb), CO (0.1 ppm), NO_2 (ppb), SO_2 (ppb), and PM_{10} ($\mu g\,m^{-3}$) under the MEK four land-use types of **(a)** residence, **(b)** commerce, **(c)** industry, and **(d)** greenbelt.

ACPD
15, 16985–17050, 2015

CC BY

ACPD

15, 16985–17050, 2015

Spatiotemporal variations of air pollutants with land-use types

J.-M. Yoo et al.

CC BY

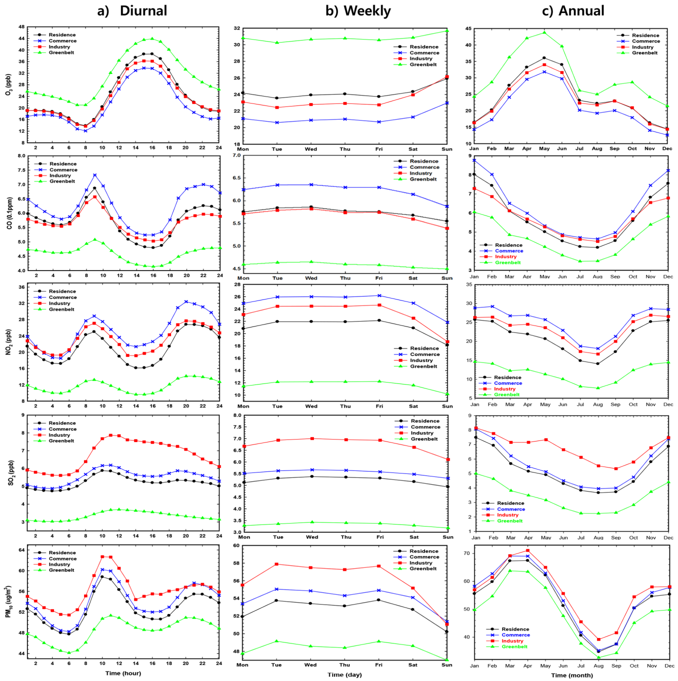

Figure 6. The **(a)** diurnal, **(b)** weekly, and **(c)** annual variations in a 0.25° × 0.25° grid of the O_3 (ppb), CO (0.1 ppm), NO (ppb), SO_2, (ppb) and PM_{10} (µg m^{-3}) observations over South Korea during 2002–2013 under the MEK four land-use types as follows: residence (black circle), commerce (blue cross), industry (red square) and greenbelt (green triangle).

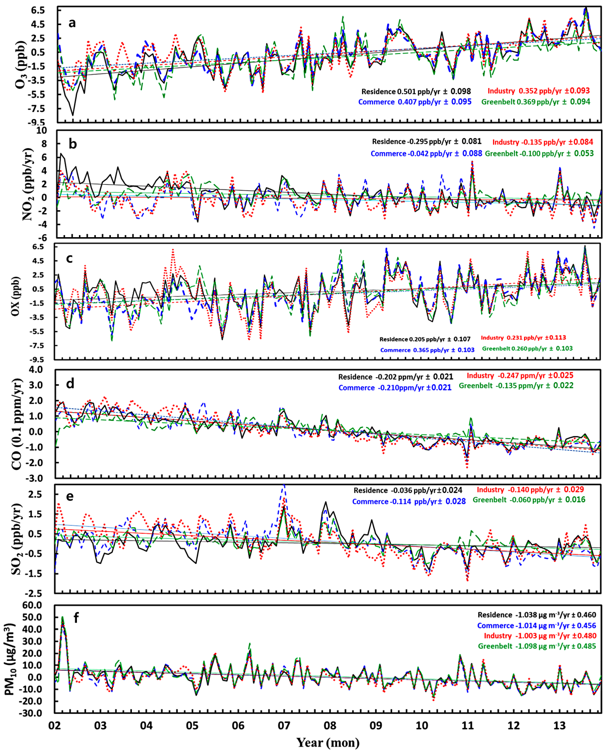

Figure 7. Time series of the monthly surface air pollutant anomalies in a 0.25° × 0.25° grid of the **(a)** O_3 (ppb), **(b)** NO_2 (ppb) **(c)** OX (ppb), **(d)** CO (0.1 ppm), **(e)** SO_2 (ppb), and **(f)** PM_{10} ($\mu g\,m^{-3}$) observations over South Korea during the period from January 2002 to December 2013 under the following MEK land-use types; residence (black solid), commerce (blue dashed), industry (red dotted) and greenbelt (green dashed). The ± trend values define the 95 % confidence intervals.

ACPD
15, 16985–17050, 2015

cc BY

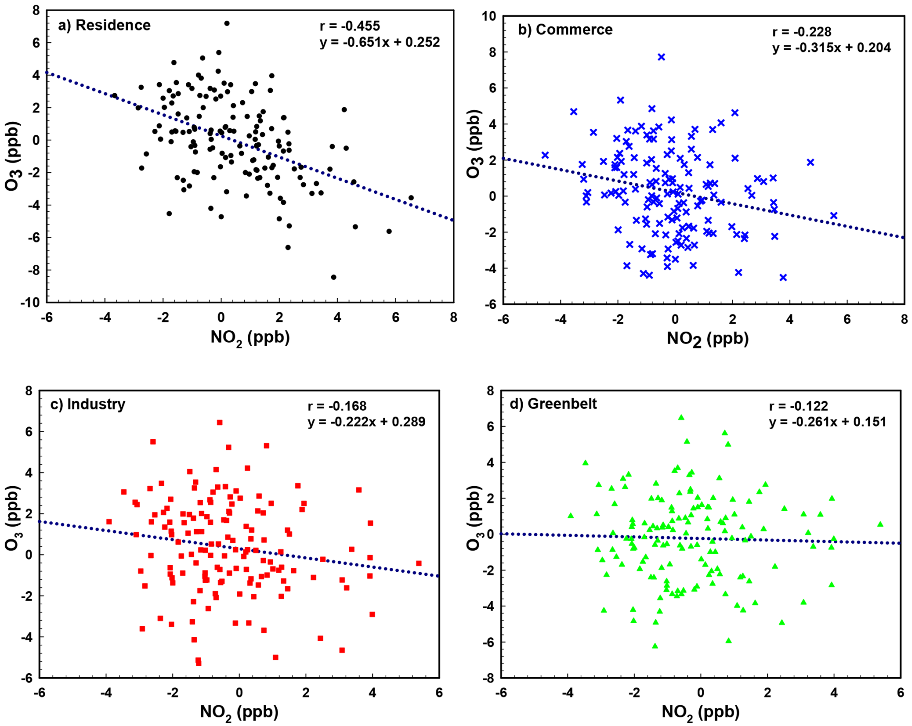

Figure 8. Scatter diagrams of the monthly anomalies of O_3 (ppb) vs. NO_2 (ppb) in South Korea during the period from January 2002 to December 2013 under the four land-use types; **(a)** residence (black circle), **(b)** commerce (blue cross), **(c)** industry (red square), and **(d)** greenbelt (green triangle). The correlation coefficient (r) and the regression dotted line are also given.

ACPD
15, 16985–17050, 2015

Spatiotemporal variations of air pollutants with land-use types

J.-M. Yoo et al.

CC BY

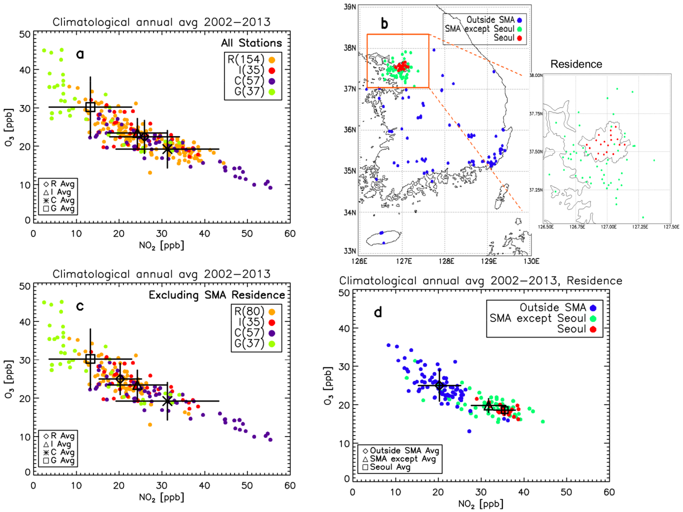

Figure 9. Climatological annual averages of the O_3 (ppb) vs. NO_2 (ppb) over South Korea during 2002–2013 under the MEK four land-use types of residence (R), commerce (C), industry (I), and greenbelt (G). **(a)** O_3 vs. NO_2 at whole 283 stations in South Korea. The number in the upper-right side panel of the figure indicates the count of stations. **(b)** Locations of 154 "residence-type" stations subdivided by the three regions as follows; (i) Seoul (red circle), (ii) the Seoul Metropolitan Area (SMA; green circle) except for Seoul, and (iii) outside of the SMA (blue circle). The rectangular area in **(b)** indicates that the SMA has been enlarged on the right side. **(c)** Same as Fig. 9a except for excluding the O_3 and NO_2 observations of the SMA residential region. **(d)** Same as **(a)** except for using the O_3 and NO_2 only in the "residence" type under the three different regions of Fig. 9b. The mean values and standard deviations for the annual values of NO_2 and O_3 in each of the types are indicated in (**a**, **b**, and **d**).

ACPD
15, 16985–17050, 2015

Spatiotemporal variations of air pollutants with land-use types

J.-M. Yoo et al.

CC BY

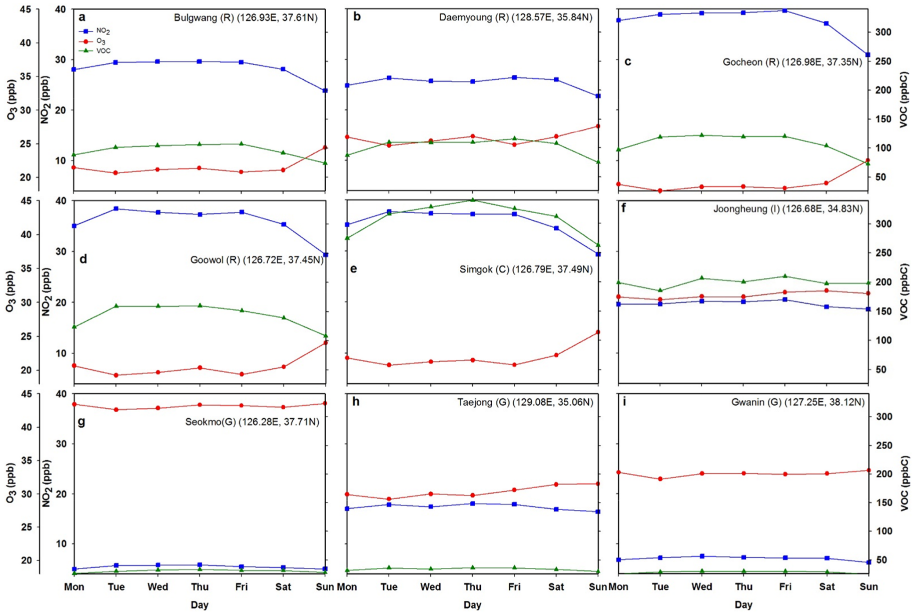

Figure 10. The weekly variations in the VOCs (green triangle), O_3 (red square), and NO_2 (blue rectangle) concentrations at the 9 photochemical air pollution monitoring stations in South Korea since 2007 under the MEK four land-use types as follows; residence (R), commerce (C), industry (I), and greenbelt (G). Please see Table 1 for the observational period at each of the VOCs station. For convenience, the terminology of "VOC" in the figures means "VOCs" in the text.

ACPD
15, 16985–17050, 2015

CC BY

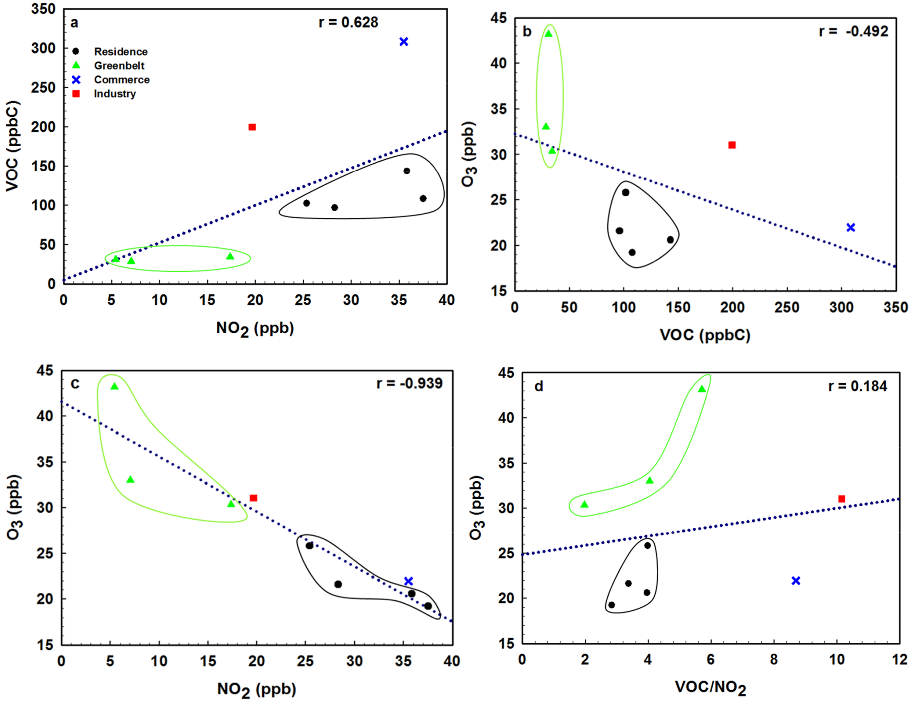

Figure 11. Scatter diagrams of the long-term averages of **(a)** VOCs vs. NO_2, **(b)** O_3 vs. VOCs, **(c)** O_3 vs. NO_2, and **(d)** O_3 vs. the ratio of VOCs/NO_2 at 9 of the photochemical air pollution monitoring stations over South Korea since 2007 under the following four land-use types; residence (black circle), commerce (blue cross), industry (red square), and greenbelt (green triangle). The correlation coefficient (*r*) and the regression dotted line were also given.

CC BY

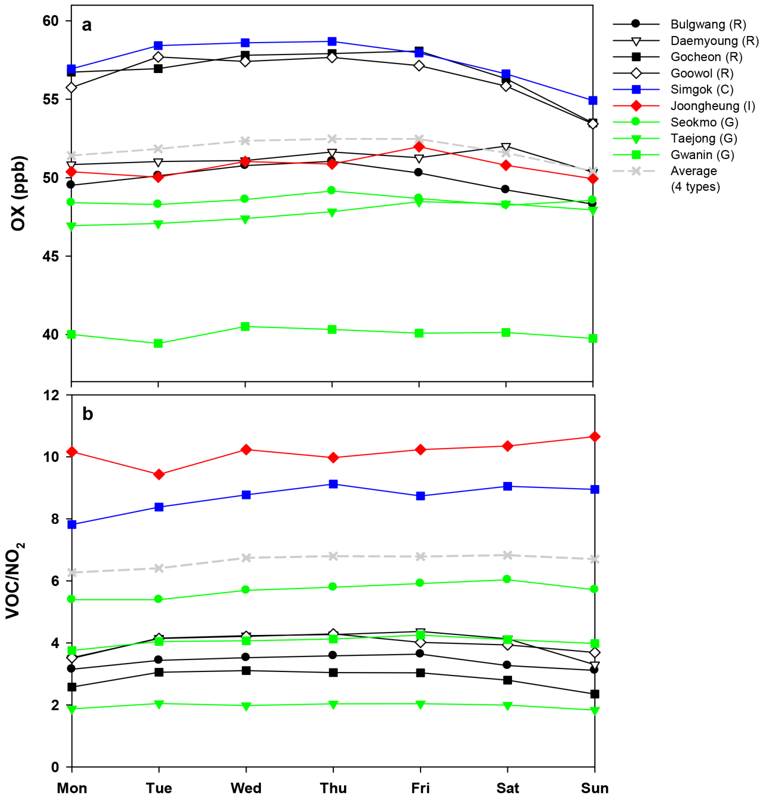

Figure 12. Weekly variations in the **(a)** OX and **(b)** VOCs/NO_2 values 2007 at nine of the photochemical air pollution monitoring stations of the MEK in South Korea. Please see Table 2 for the observational period at each of the VOCs stations.

CC BY

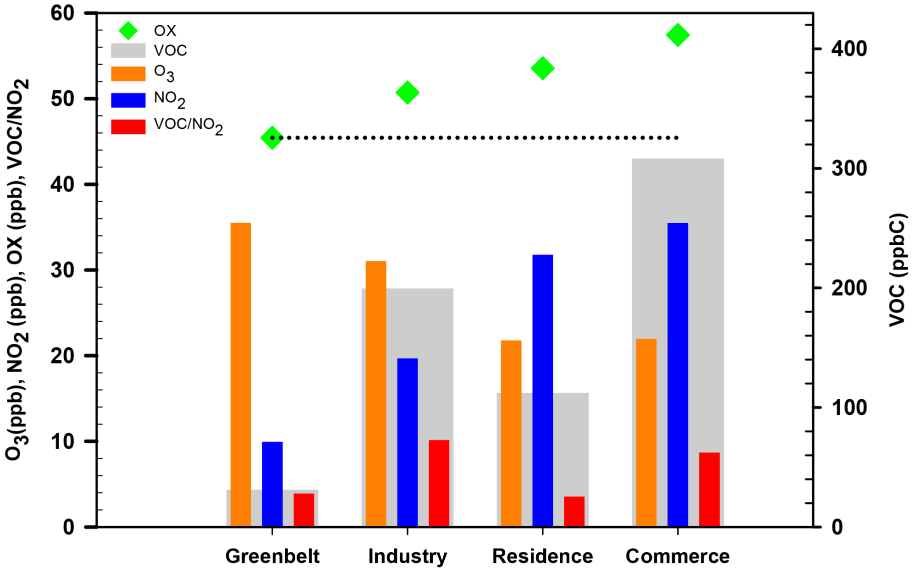

Figure 13. Climatological averages of the OX (ppb), VOCs (ppbC), O_3 (ppb), NO_2 (ppb) and the ratio of VOCs/NO_2. The values of the VOCs, O_3, NO_2, and the ratio in the bar graph are shown in the colors of grey, scalet, blue and red, respectively, at 9 of the photochemical air pollution monitoring stations over South Korea since 2007 under the following MEK four land-use types of residence, commerce, industry, and greenbelt. The OX values are presented as green diamonds. Please see Table 2 for the observational period at each of the VOCs station.

ACPD
15, 16985–17050, 2015